THERMAL NEUTRON CAPTURE IN BROMINE

BY

HAILU GEREMEW

SUBMITTED IN PARTIAL FULFILLMENT OF THE

REQUIREMENTS FOR THE DEGREE OF

MASTER OF SCIENCE IN PHYSICS

AT

ADDIS ABABA UNIVERSITY

ADDIS ABABA, ETHIOPIA

March 2012

ADDIS ABABA UNIVERSITY

DEPARTMENT OF

PHYSICS

The undersigned hereby certify that they have read and recommend to the School of Graduate Studies for acceptance a thesis entitled “Thermal neutron capture in Bromine” by Hailu Geremew Zeleke in partial fulfillment of the requirements for the degree of Master of Science in Physics.

Dated: March 2012

Advisor: _____

Prof.A.K.Chaubey

Examiners: _____

Dr. S. Bhatnagar

_____

Dr. Tilahun Tesfaye

ADDIS ABABA UNIVERSITY

Date: March 2012

Author: HAILU GEREMEW

Title: *THERMAL NEUTRON CAPTURE IN BROMINE*

Department: Physics

Degree: M.Sc. Convocation: March Year: 2012

Permission is herewith granted to Addis Ababa University to circulate and to have copied for non-commercial purposes, at its discretion, the above title upon the request of individuals or institutions.

_____

Signature of Author

TABLE OF CONTENTS**********PAGE

*List of figures********** pages*

*List of tables**********pages*

*List of graphs**********pages*

Abstract

In this thesis, the build-up and decay of radioactivity in two stable isotopes of Bromine caused by reaction with slow neutrons will be studied. In particular, we will be able to measure the radioisotope capture cross section of these samples, using HPGe-detector and beta-counter on the decay of radioactivity data taken. For the decay of Br-82 the ground state thermal neutron cross section *0.2565±0.023barn* by using High purified Germanium detector and for Br-80 decay the ground state thermal neutron cross section *8.653±0.78barn* by using beta counter were observed from this work and the total thermal neutron cross section for the two isotopes obtained from the measurement were compared with the calculated theoretical values.

Acknowledgment

Some grateful acknowledgments are certainly stated in the following manner for those who assist my graduate study in deferent aspects.

Above all my innocent heavenly father, the God for his graceful help to cope with my challenges. A number of colleagues and families devoted a great deal of their time for encouragement and their financial resources. In this respect, I would like to thanks Ato Yihunie Hibstie, Getu Ferenji and all my Families.

Finally, I am very grateful to prof. A.K. Chaubey (advisor), who is most closely associated with this thesis, for his all round help and kindness.

Addis Ababa University Hailu Geremew

Chapter One

Introduction

Neutron reactions can be divided with respect to neutron energy in to three classes; thermal, epithermal and fast. Thermal neutrons have approximately a Maxwellian energy distribution having mean energy of 0.025ev. Fast neutrons come directly from fission, having energies up to 20 MeV. The epithermal are partially moderated neutrons with an energy range between about 0.1Mev and near thermal energies. Among heavy elements thermal and epithermal neutrons can cause **(**n,α) and (n, p) reactions, as well as neutron capture, depending on the energies for the various particles. Among heavier elements the neutron result primarily in capture (n,γ) and fission reactions, fast neutrons being required for particle emission reaction such as (n, 2n), (n, p), and emission of high energy neutrons. In chapter two the theoretical study of neutron induced reaction will be seen where as in chapter three the experimental results will be observed.

The objective of this thesis is to study thermal neutron induced reaction (n,γ) using the two stable isotopes of bromine (Br-79 and Br-81) and measure its cross section. The decay of radioactive isotope induced by thermal neutron for bromine and two different masses of iodine, which is used to determine flux of thermal neutron induced reaction in bromine, will be seen. The probability of a neutron interacting with nucleus for a particular reaction is dependent upon not only the kind of nucleus involved, but also the energy of neutron. Accordingly, the absorption of thermal neutrons in most material is much more probable than the absorption of a fast neutron. Also, the probability of interaction will vary depending up on the type of interaction involved.

The probability of a particular interaction occurring between a neutron and a nucleus is called *the microscopic cross section* (σ) of the nucleus for the particular interaction. This cross section will vary with the energy of the neutron. Microscopic cross section is the effective area of the nucleus presented to the projectile that if projectile passes through this the reaction will take place. The larger the effective area is the larger the probability of interaction. Because the microscopic cross section has definition of an area, it is expressed in unit of area, or square centimeters. A square centimeter is large compared to the effective area of a nucleus; hence it is expressed in a smaller unit of area called a barn, which is 10^{-24} cm^2.

Bromine is found in the periodic table of elements in group seven, which has more than 30 isotopes and out of this two are stable available in nature 49.31%, Br-81 and 50.69%, Br-79. Since bromine is unstable in nature (salt maker), potassium bromide is used in this study.

Irradiating sample of potassium bromide and two potassium iodides by a uniform neutron beam and measuring the induced radioactivity by counting gamma ray and beta particles using High Purity Germanium detector calibrated by Europium source and pre-calibrated beta counter, thermal neutron capture cross section of Br-81 and Br-79 respectively will be measured. To perform this experiment, standard sources (Eu or other source) for the calibration of the detector, thermal neutron source to have beam of thermal neutrons for the activation of the sample of the isotope, the respective detector; High Purity Germanium detector and beta counter are the main used materials in nuclear laboratory of AAU.

Chapter Two

Theoretical approaches of neutron capture cross section

2.1. Basic Properties of the Neutron

The neutron is a subatomic particle with zero charge, mass m = 1.0087 atomic mass units, spin $1/2$, and magnetic moment μ_n = -1.9132 nuclear magnetons. These four properties combine to make the neutron a highly effective probe of matter. The zero charge means that its interactions with matter are confined to the short-ranged nuclear and magnetic interactions, which in turn has *two* important consequences: the interaction probability is small, so the neutron can usually penetrate into the bulk of a sample and, as we shall see, it can be described in terms of the first Born approximation and thus given in explicit form by quite simple formulas.

If one considers the wave nature of the neutron, it can be described by a wavelength λ given by;

$$h^2/2m_n\lambda^2 = kT \qquad 1$$

where h is Planck's constant, T is temperature of the moderator. For the value of neutron mass and for T ≈ 300 K, λ ≈ 2 $\overset{0}{A}$ (2 x 10^{-8} cm), a distance comparable to the mean atomic separation in a solid or dense fluid. Furthermore, the kinetic energy of such neutrons is on the order of 0.025 eV. Thus, both wavelength and energy are ideally suited to the probing, in which simultaneous transfer of momentum and energy is observed. The magnetic moment of the neutron makes it a unique probe of magnetism on an atomic scale: neutrons may be scattered from the magnetic moments associated with unpaired electron spins in magnetic samples. [1]

2.2. Elements and isotopes

The structure of the nucleus was unknown when Bohr proposed his atomic model. It soon became apparent, however, with experimental proof arriving thanks to Chadwick in 1932, that nuclei comprised two types of particle: protons and neutrons, collectively known as *nucleons*.

– The *proton* is 1836 times heavier than the electron, and has a positive electric charge.

– The *neutron* has almost the same mass (1839 times heavier than the electron), but carries no electric charge.

Different combinations of Z and N_n (number of neutrons) are called *nuclides*. Nuclides with the same mass number are called *isobars*. Nuclides with the same value of N_n are called *isotones*. Each element is characterized by the protons number (*Z),* (which is also the number of electrons), and we often find that different atoms of the same element have a different number of neutrons (N), accompanying the protons in the nucleus. These are *isotopes*. This word means "*same place*", and indicates that these different atoms occupy the same position in the Periodic Table. Most elements have a few stable isotopes and several unstable, radioactive isotopes. [2],[3]

For example, Bromine (Br Z=35) in nature consists of two stable isotopes, ^{79}Br (50.69 percent) and ^{81}Br (49.31 percent), and at least more than 30 radioactive isotopes. A radioactive isotope is one that breaks apart and gives off some form of radiation. Radioactive isotopes are produced when very small particles are fired at atoms. Bromine is toxic if inhaled or swallowed. It can damage the respiratory system and the digestive system, and can even cause death. It can also cause damage if spilled on the skin. It is too reactive to exist as a free element in nature. Instead, it occurs in compounds, the most common of which are sodium bromide (NaBr) and potassium bromide (KBr). These compounds are found in seawater and underground salt beds. These salt beds were formed in regions where oceans once covered the land and when the oceans evaporated (dried up), it left behind. [4]

2.3. Neutron Activation Analysis (NAA)

Neutron activation analysis is a sensitive multi-element analytical technique used for both qualitative and quantitative analysis of major, minor, trace and rare elements. NAA was discovered in 1936 by *Hevesy* and *Levi,* who found that samples containing certain rare earth elements became highly radioactive after exposure to a source of neutrons.[5]

In the analysis, stable nuclei in the sample undergo neutron induced nuclear reactions when the sample is exposed to a flux of neutrons.

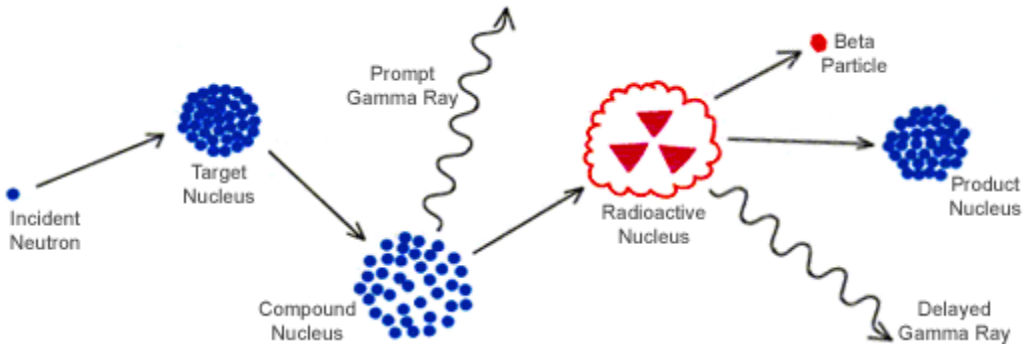

Fig. 1: Capture of neutron by target nucleus

The most common neutron reaction is neutron capture by a stable nucleus that produces a radioactive nucleus. The "neutron rich" radioactive nucleus then decays, with a unique half-life, by the emission of a beta particle. In the vast majority of cases, gamma-rays are also emitted in the beta decay process and a high-resolution gamma-ray spectrometer is used to detect these "delayed" gamma rays from the artificially induced radioactivity in the sample for both qualitative and quantitative analysis. The energies of the delayed gamma rays are used to determine which elements are present in the sample, and the number of gamma rays of a specific energy is used to determine the amount of an element in the sample.[6]

Thermal Neutron Analysis (TNA) relies on the capture of low-energy *(thermal)* neutrons and the subsequent release of detectable radiation by certain isotopes of some chemical elements. It should not be confused with the technique of neutron thermalisation which is fundamentally different.[7]

2.3.1. Principles of Neutron Activation Analysis (NAA)

The (n,γ) reaction is the fundamental reaction for neutron activation analysis. The probability of a neutron interacting with a nucleus is a function of the neutron energy. This probability is referred to as the capture cross-section, and each nuclide has its own neutron energy capture cross-section relationship. For many nuclides, the capture cross-section is greatest for low energy neutrons (referred to as thermal neutrons). The activity for a particular radionuclide, at any time t during an irradiation, can be calculated from the following, equation.

$$A_t = \sigma_{act} \varphi N(1 - e^{-\lambda t}) \quad (2)$$

where A_t = the activity in number of decays per unit time,

σ_{act} = the activation cross-section,

φ = the neutron flux (usually given in number of neutrons cm^{-2} s^{-1}),

N = the number of parent atoms,

λ = the decay constant (number of decays per unit time), and

t = the irradiation time.

Note that for any particular radioactive nuclide radioactive decay is occurring during irradiation, hence the total activity is determined by the *rate of production minus the rate of decay*. If the irradiation time is much longer than the half-life of the nuclide, saturation is achieved. What this means is that the rate of production and decay is now in equilibrium and further irradiation will not lead to an increase in activity. The optimum irradiation time depends on the type of sample and the elements of interest. Because the neutron flux is not constant, the total flux (called fluence) received by each sample must be determined using an internal or external fluence monitor. It is sometimes useful to convert from half-life to decay constant. This can be done using the following equation;

$$t_{1/2} = 0.693/\lambda \quad (3)$$

where $t_{1/2}$ is the half-life and λ is the decay constant. With some notable exceptions the half-lives earlier in the decay chain tend to be shorter than those occurring later. Each radioactive nuclide is also decaying during the counting interval and corrections must be made for this decay. The standard form of the radioactivity decay correction is;

$$A = A_0 e^{-\lambda t} \quad (4)$$

where A is the activity at any time t, A_o is the initial activity, λ is the decay constant and t is time.[8]

The principle of NAA is applicable for elements:

- Whose pair nucleus is available (stable) and natural abundance is large.
- The next isotope produced must be radioactive with measurable half life, neither too short nor too long.
- The decay scheme of radioactive nuclei produced must be well known.

One can derive expression for reaction cross section (n,γ) reaction as;

$$\sigma = \frac{(dn/dt)\exp(\lambda t_2)}{N_0 \phi \varepsilon_G \theta k (1-\exp(-\lambda t_1))(1-\exp(-\lambda t_3))} \quad 5$$

Where dn/dt , is activity of isotope produced.

N_0 is number of nuclei of the element to be activated given as;

$$N_0 = \frac{mNf}{A} \quad 6$$

Where m=mass(in mass unit)

N=Avogadro number

f=natural abundance of isotopes

A=atomic weight

ϕ is flux of thermal neutron,

ε_G is geometry dependent efficiency of gamma ray of interest,

θ is percentage intensity of gamma ray,

K is self absorption coefficient for gamma ray absorption in the sample and

t_1, t_2, t_3 are time of irradiation, after the stop of irradiation and start of counting and time for the counting activity respectively.[9]

- ***Advantages of NAA***

Pulse neutron sources (also called pulse neutron generators) have found a number of applications in science, industry, medicine, and technology. To name a few:

- *Real-time analysis of bulk materials:* Materials such as cement and coal moving on conveyor belts are examples of bulk materials that are extensively examined by applying fast and thermal neutron beams for activation analyses.

- *Detection of explosive, chemical and nuclear materials:* Such materials may be accurately detected for fast security checks of airline-cargo or other unknown packages.

- *Medical applications:* An accurate and simple measurement of the body's fat is achieved using neutron pulse generators. The measurement is based on neutron interactions with carbon and oxygen. [10]

- ***Disadvantages of NAA***

-*The technique requires access to a high-flux neutron source,* to obtain the sensitivities of target that, the techniques cannot be performed “in house” by industry.

-*Time required for the analysis.* Given the continuous production schedules on which the semiconductor industry operates, an analytical protocol that takes four to five weeks can be inconvenient.

-*It cannot provide information on some of the light elements,* particularly B, C, O and Al, that are monitored to ensure optimum performance of semiconductor devices. [6]

2.4. Neutron production

Neutrons are produced from neutron sources such as a nuclear reactor, a radioactive, or an accelerator-based source. However, the complexity of a reactor and the systems involved as well as the cost make simple and broad use of reactors impractical for small scale industrial, medical, or research applications. On the other hand, radioactive neutron sources are used in an innumerable amount of industrial applications and are ideal when a continuous source is needed. However, such a source is not appropriate for applications that require neutrons of a specific energy or emission of neutrons in specified time pulses. One example of a large accelerator-based neutron source is the Spallation Neutron Source under construction at Oak Ridge National Laboratory in the United States.

2.4.1. A nuclear reactor

It is the most inexhaustible source for the production of neutrons of all energies. For example if we consider elements that contain large atoms (typically uranium-235, uranium-238, or plutonium-239) that are inherently unstable, these atoms undergo nuclear fission process and by this process two or three neutrons and approximately 200MeV of heat energy are emitted. These neutrons leave the nucleus with moderately high kinetic energy and are referred to as fast neutrons. These neutrons are slowed with a moderator such as graphite, water, or heavy water. These are called 'very slow' or thermal neutrons, and to a lesser extent the fast neutrons, in turn impact other fissionable atoms causing their fission, and so forth. The interaction of single neutron with Uranium (235) will gives two neutrons with high energy and living Zr and Te as a product.

$$ {}_{0}^{1}n + {}_{92}^{235}U \longrightarrow {}_{40}^{98}Zr + {}_{52}^{135}Te + 2{}_{0}^{1}n + Energy(200MeV) \quad [10] $$

2.4.2. Radioactive neutron sources

Radioactive neutron sources are important in the laboratory. They are small and portable, they have a constant output, and they require no maintenance. They are used often in the study of the slowing down and diffusion of neutron in various media as well as in the determination of neutron scattering and absorption cross sections.

a) Using alpha neutron sources

Many alpha-neutron reactions have been observed, only a few, those with the highest neutron yields, have generally been used in the preparation of neutron sources. It may be expected from the general properties of nuclei that other (α,n) reaction which lead to final nuclei of even Z(proton number) and even N(neutron number)would give high yields.

In the lighter elements the energy spectrum of the emitted neutrons is usually determined by the excitation function and by the probabilities of leaving the residual nucleus in a small number of excited states. To consider the more important reactions;

$$ Be^{9} + He^{4} \text{----------} > C^{12} + n + 5.708MeV $$

$$ B^{11} + He^{4} \text{----------} > N^{14} + n + 0.5MeV $$

The corresponding reaction for B^{10} is,

$B^{10} + He^4$----------->$N^{13} + n + 1.07MeV$

Some of the low energy neutrons are probably associated with the multibody break up processes,

$He^4 + Be^9$----------->$He^4 + Be^8 + n - 1.666MeV$

----------> $3He^4 + n - 1.572MeV$ [11]

b) *Using gamma neutron source*

Neutrons can also be produced in the reaction of γ rays with targets most commonly made of beryllium or deuterium (for example heavy water). Such reactions are referred to as *photo neutron sources*. The binding energy of the neutrons in these light elements is low and a large amount of energy is therefore not required for the reaction to occur.

$$^{9}Be(\gamma,n)^{8}Be - - - - - - - - - - - - - - - - - > Q = 1.63MeV$$

$$^{2}H(\gamma,n)^{1}H - > Q = 2.23MeV$$

Neutrons produced by photodisintegration of nuclei are *mono energetic* and such sources are reproducible (in terms of neutron energy). The most common sources of γ rays used for these interactions are the γ rays emitted in radioactive decays of $^{24}Na(E_\gamma = 2.8MeV, T_{1/2} = 15hours)$ Or $^{124}Sb(E_\gamma = 1.67MeV, T_{1/2} = 60.9days)$.

Any gamma source emitting gamma rays of energy greater than half life of the source will depend up on the half life of gamma emitter elements. Most probably this gamma-neutron source is used for the production of *thermal neutron* and other neutrons having *energy spectra* are thermalized by wax.

2.4.3. Accelerator-based neutron source

The flux of neutron produced from the radioactive source is small. In place of radioactive source if accelerators are used very intense beam can be produced, because these can be focused using *focusing electrodes* and *accelerated by accelerating voltage* to a desired energy.

For example, using alpha as accelerated charged particle (using cyclotron machine) and Beryllium as a target neutrons of various mono energy can be produced.

a) Small scale neutron producing accelerator

A small scale accelerators and compact pulse neutron sources use nuclear reactions to produce neutrons. The most common are the deuterium-deuterium ($^2H-^2H$) and deuterium-tritium ($^2H-^3H$) reactions

$^3H(^2H,n)^4He$ ----------> Q=17.59 MeV

$^2H(^2H,n)^3He$ ----------> Q=3.27 MeV

These reactions produce 14.1 MeV and 2.5 MeV energy neutrons, respectively. [10]

b) Large scale neutron producing accelerator (spallation)

Most fundamental neutron physics experiments are conducted with slow neutrons for two main reasons:

- First, slower neutrons spend more time in an apparatus.
- Second, slower neutrons can be more effectively manipulated through coherent interactions with matter and external fields.

Free neutrons are usually created through either *fission reactions* in a nuclear reactor or through *spallation*.

In the spallation process, *protons* (typically) are accelerated to energies in the GeV range and strike a high Z target, producing approximately *20* neutrons per proton with energies in the *fast* and *epithermal* region. This is an order of magnitude *more* neutrons per nuclear reaction than from fission. To maximize the neutron density in fission process, it is necessary to increase the *fission rate per unit volume*, but the power density is ultimately limited by heat transfer and material properties. Although the time-averaged fluence from spallation neutron sources is presently about an order of magnitude lower than for fission reactors. The main feature that differentiates spallation sources from reactors is *their convenient operation in a pulsed mode*. At most reactors one obtains continuous beams with a thermalized Maxwellian energy spectrum. In a pulsed spallation source, neutrons arrive at the experiment while the production source is *off,* and the frequency of the pulsed source can be chosen so that slow neutron energies can be determined by *time-of-flight methods*. [12]

2.4.4. Neutron Multiplication

The two or three neutrons born with each fission undergo a number of scattering collisions with nuclei before ending their lives in absorption collisions, which in many cases cause the absorbing nucleus to become radioactive. If the neutron is absorbed in a fissionable material, frequently it will cause the nucleus to fission and give birth to neutrons of the next generation. Since this process may then be repeated to create successive generations of neutrons, a neutron chain reaction is said to exist. We characterize this process by defining the chain reaction's multiplication, *k*, as the ratio of fission neutrons born in one generation to those born in the preceding generation.

Suppose at some time, say t=0, we have no neutrons produced by fission; we shall call these the *zeroth* generation. Then the first generation will contain kn_o neutrons, the second generation $k^2 n_0$, and so on: the i^{th} generation will contain $k^i n_0$. On average, the time at which the i^{th} generation is born will be $t = i.l$; where l is the neutron life time. We can eliminate i between these expressions to estimate the number of neutrons present at time t:

$$n(t) = n_0 k^{t/l} \qquad 7$$

Thus the neutron population will increase, decrease, or remain the same according to whether *k* is *greater than*, *less than*, or *equal to one*. The system is then said to be *supercritical, subcritical,* or *critical*, respectively.

A more widely used form of the Eq.7 results if we limit our attention to situations where *k* is close to one. First note that the exponential and natural logarithm are inverse functions. Thus for any quantity, say *x*, we can write *x = exp[ln(x)]*. Thus with $x = k^{t/l}$ we may write the Eq.7 as:

$$n(t) = n_0 \exp[(t/l)\ln(k)] \qquad 8$$

If *k* is close to one, that is, |k-1|<<1, we may expand *ln(k)* about 1 as *ln(k)~ k-1*, to yield:

$$n(t) = n_0 \exp[(k-1)t/l] \qquad 9$$

2.4.5. Fission Products

Fission results in many different pairs of fission fragments. In most cases one has a substantially heavier mass than the other. For example, a typical fission reaction is:

$$n + {}^{235}_{92}U \text{ ---------->} {}^{140}_{54}Xe + {}^{94}_{38}Sr + 2n + 200MeV.$$

Fission fragments are unstable because they have neutron to proton ratios that are too large.

Nearly all of the fission products fall into *two* broad groups. The *light group* has mass numbers between 80 and 110, whereas the *heavy group* has mass numbers between 125 and 155. Roughly *8%* of the 200MeV of energy produced from fission is attributable to the *beta decay* of fission products and the *gamma rays* associated with it.

Fissile and Fertile Materials

In discussing nuclear reactors we must distinguish between two classes of fissionable materials:

- *A fissile material* is one that will undergo fission when bombarded by neutrons of *any* energy. The isotope uranium-235 is a fissile material.
- *A fertile material* is one that will capture a neutron, and transmute by radioactive decay into a fissile material. Uranium-238 is a fertile material.

Fertile isotopes may also undergo fission directly, but only if impacted by a *high energy neutron*, typically in the *MeV* range. Thus fissile and fertile materials together are defined as *fissionable materials.* Fertile materials by themselves, however, are not capable of sustaining a chain reaction. There is a neutron that initiate, which occurs naturally as the result of very high-energy cosmic rays colliding with nuclei and causing neutrons to be ejected. If other source (Am-Be source)* were not present these would trigger a chain reaction. [13]

2.5. NEUTRON INTERACTIONS

Neutrons can cause many different types of *interactions,* which can be divided with respect to *its energy* in to *three* classes; *thermal, epithermal and fast*. The neutron may simply scatter off the nucleus in two different ways, or it may actually be absorbed into the nucleus. If a neutron is absorbed into the nucleus, it may result in the emission of a gamma ray or a subatomic particle, or it may cause the nucleus to fission.

Scattering

A neutron *scattering* reaction occurs when a nucleus, after having been struck by a neutron, emits a single neutron. Despite the fact that the initial and final neutrons do not need to be (and often are not) the same, the net effect of the reaction is as if the projectile neutron had merely "bounced off," or scattered from, the nucleus. The two categories of scattering reactions, elastic and inelastic scattering are described in the following paragraphs.

2.5.1. Elastic Scattering

In an *elastic scattering* reaction between a neutron and a target nucleus, there is *no appreciable energy transferred* into nuclear excitation. Momentum and kinetic energy of the "system" are conserved although there is usually some transfer of kinetic energy from the neutron to the target nucleus. The target nucleus gains the amount of kinetic energy that the neutron loses.

In the elastic scattering reaction, the conservation of momentum and kinetic energy is represented by the equations below.

Conservation of momentum (mv)

$$(m_n.v_{ni}) + (m_t.v_{ti}) = (m_n.v_{nf}) + (m_t.v_{tf}) \qquad 10$$

Conservation of kinetic energy ($^1/2\ mv^2$)

$$(\frac{1}{2}m_n v_{ni}^{\ 2}) + (\frac{1}{2}m_t v_{ti}^{\ 2}) = (\frac{1}{2}m_n v_{nf}^{\ 2}) + (\frac{1}{2}m_t v_{tf}^{\ 2}) \qquad 11$$

where:

m_n = mass of the neutron

m_t = mass of the target nucleus

v_{ni} = initial neutron velocity

v_{nf} = final neutron velocity

v_{ti} = initial target velocity

v_{tf} = final target velocity

Elastic scattering of neutrons by nuclei can occur in *two* ways. The more unusual of the two interactions is the absorption of the neutron, forming a compound nucleus, followed by the re-*emission of a neutron* in such a way that the total kinetic energy is conserved and the nucleus returns to its ground state. This is known as *resonance elastic scattering* and is very dependent upon the initial kinetic energy possessed by the neutron. Due to formation of the compound nucleus, it is also referred to as *compound elastic scattering*. The second, more usual method is termed *potential elastic scattering* and can be understood by visualizing the neutrons and nuclei to be much like billiard balls with impenetrable surfaces. Potential scattering takes place with incident neutrons that have an energy of up to about 1 MeV. In potential scattering, the neutron *does not actually touch* the nucleus and a *compound nucleus is not formed*. Instead, the neutron is acted on and scattered by the *short range nuclear forces* when it approaches close enough to the nucleus.

2.5.2. Inelastic Scattering

In an *inelastic scattering*, the incident neutron is absorbed by the target nucleus, forming a compound nucleus. The compound nucleus will then emit a neutron of lower kinetic energy which leaves the original nucleus in an excited state. The nucleus will usually, by one or more *gamma emissions*, emit this excess energy to reach its ground state.

Absorption Reactions

Most *absorption reactions* result in the loss of a neutron coupled with the production of a charged particle or gamma ray. When the product nucleus is radioactive, additional radiation is emitted at some later time. Radiative capture, particle ejection, and fission are all categorized as absorption reactions and are briefly described below.

-*Radiative capture:* the incident neutron enters the target nucleus forming a compound nucleus. The compound nucleus then decays to its ground state by gamma emission. An example of a radiative capture reaction is shown below.

$$ {}^{1}_{0}n + {}^{238}_{92}U \longrightarrow ({}^{239}_{92}U)^{*} \longrightarrow {}^{239}_{92}U + {}^{0}_{0}\gamma $$

-*Particle ejection:* the incident particle enters the target nucleus forming a compound nucleus. The newly formed compound nucleus has been excited to a high enough energy level to cause it to eject a new particle while the incident neutron remains in the nucleus. After the new particle is ejected, the remaining nucleus may or may not exist in an excited state depending upon the mass-energy balance of the reaction. An example of a particle ejection reaction is shown below.

$$ {}^{1}_{0}n + {}^{10}_{5}B \longrightarrow ({}^{11}_{5}B)^{*} \longrightarrow {}^{7}_{3}Li + {}^{4}_{2}\alpha $$

-*Fission:* the incident neutron enters the heavy target nucleus, forming a compound nucleus that is excited to such a high energy level ($E_{exc} > E_{crit}$) that the nucleus "splits" (fissions) into two large fragments plus some neutrons. An example of a typical fission reaction is shown below.

$$ {}^{1}_{0}n + {}^{235}_{92}U \longrightarrow ({}^{236}_{92}U)^{*} \longrightarrow {}^{140}_{55}Cs + {}^{93}_{37}Rb + 3({}^{1}_{0}n) $$ [14]

2.5.3. Neutron Energy Spectra

The distribution of neutrons in energy is determined largely by the competition between *scattering* and *absorption* reactions. For neutrons with energies significantly above the thermal range, a scattering collision results in degradation of the neutron energy, whereas neutrons in thermal equilibrium have near equal probabilities of gaining or losing energy when interacting with the thermal motions of the nuclei that constitute the surrounding medium. In a medium for which the average energy loss per collision and the ratio of scattering to absorption cross section are both large, the neutron distribution in energy will be close to thermal equilibrium and is then referred to as *a soft or thermal spectrum*. Conversely in a system with small ratios of neutron degradation to absorption, neutrons are absorbed before significant slowing down takes place. The neutron distribution then lies closer to the fission spectrum and is said to be *hard or fast*.

The neutron distribution may be expressed in terms of the density distribution;

$N(E)dE$=number of neutrons/cm^{3}with energy between E and $E+dE$, 12

which means that

$$N=\int_0^\infty N(E)dE \text{ =total number of neutrons/cm}^3 \quad 13$$

The more frequently used quantity, however, is the neutron flux distribution defined by

$$\varphi(E)=v(E)N(E) \quad 14$$

where v(E) is the neutron speed corresponding to kinetic energy E.

The flux, often called the scalar flux, has the following physical interpretation:

- ✪ $\varphi(E)dE$ is the total distance traveled during one second by all neutrons with energies between E and E+dE located in 1 cm^3.

Likewise, we may interpret the macroscopic cross section as;

$\sum_x(E)$=Probability/cm of flight of neutron with energy E undergoing a reaction of type x. 15

Thus multiplying a cross section by the flux, we have;

$\sum_x(E)\ \varphi(E)dE$=Probable number of collision of type x/s/cm^3 for neutrons with energies b/n E and E+dE. 16

Finally, we integrate over all energy to obtain;

$$\int_0^\infty \sum_x(E)\ \varphi(E)dE \text{=Probable number of collisions of type x/s/cm}^3 \text{ of all neutrons.} \quad 17$$

This integral is referred to as a *reaction rate*, or if x=s, a, f as the scattering, absorption, or fission rate. A more quantitative understanding of neutron energy distributions results from writing

down a balance equation in terms of the neutron flux. Since $\sum(E)\varphi(E)$ is the collision rate or number of neutrons of energy E colliding/s/cm^3 each such collision removes a neutron from energy E either by absorption or by scattering to a different energy. We may thus regard it as a loss term that must be balanced by a gain of neutrons arriving at energy E. Such gains may come from fission and from scattering, where the number coming from fission will be $x(E)$, given by;

$x(E) = 0.453e^{-(1.036E)}\sinh(2.29E)$.

We next recall that the probability that a neutron that last scattered at energies between E$'$ and E$'$ + dE$'$ will be scattered to an energy E as P(E$'$-->E)dE$'$. Since the number of neutrons scattered from energy E$'$ is $\sum_s$(E$'$) φ(E$'$), the scattering contribution comes from integrating P(E$'$-->E) $\sum_s$(E$'$) φ(E$'$)dE$'$ over E$'$. The balance equation is thus;

$$\Sigma_t(E)\varphi(E) = \int P(E' -> E)\Sigma_s(E')\varphi(E')dE' + x(E)s_f \qquad 18$$

For brevity we write the foregoing equation as;

$$\Sigma_t(E)\varphi(E) = \int \Sigma_s(E' -> E)\varphi(E')dE' + x(E)s_f \qquad 19$$

where we take $\Sigma_s(E' -> E) = P(E' -> E)\Sigma_s(E')$. The balance equation is normalized by the fission term, which indicates a rate of s_f fission neutrons produced/s/cm3.

In each of the three energy ranges general restrictions apply to Eq. (19). In the thermal and intermediate ranges no fission neutrons are born and thus $x(E)$ =0. In the intermediate and fast ranges there is no up-scatter, and therefore $\Sigma_s(E' -> E) = 0$ for E$'$ < E.

2.5.4. Fast Neutrons

Over the energy range where fission neutrons are born both terms on the right of Eq. (19) contribute; near the top of that range the fission spectrum $x(E)$ dominates, since on average even one scattering collision will remove a neutron to a lower energy. In that case we may make the rough approximation,

$$\varphi(E) \approx {x(E)s_f}\Big/{\Sigma_t(E)}, \qquad 20$$

which only includes the un collided neutrons; those emitted from fission but yet to make a scattering collision. Even in the absence of moderators or other lower atomic weight materials the spectrum will be substantially degraded as a result of inelastic scattering collisions with uranium or other heavy elements. [13]

2.6. Neutron Moderators

In thermal reactors, moderator materials are required to reduce the neutron energies from the fission to the thermal range with as few collisions as possible, thus circumventing resonance capture of neutrons in uranium-238. To be an effective moderator a material must have a *low atomic weight*.

Only ξ (the mean value of the logarithm of the energy loss ratio or ln(E/E$^{'}$)) given by;

$$\xi = \overline{\ln(E/E^{'})} = \int \ln(E/E^{'})P(E->E^{'})dE^{'} \qquad 21$$

is large enough to slow neutrons down to thermal energies with relatively few collisions, where E and E$^{'}$ be the neutron energy *before* and *after* the collision respectively.

A good moderator, however, must possess additional properties. Its macroscopic scattering cross section must be sufficiently *large.* Otherwise, even though a neutron colliding with it would lose large energy, in the competition with other materials, too few moderator collisions would take place to have a significant impact on the neutron spectrum.

Thus a *second* important parameter in determining a material's value as a moderator is the *slowing down power*, defined as $\xi\Sigma_s$, where $\Sigma_s = N\sigma_s$ is the macroscopic scattering cross section.

	Slowing down decrement	Slowing down power	Slowing down ratio
Moderator	ξ	$\xi\Sigma_s$	$\xi\Sigma_s/\Sigma_a(thermal)$
H_2O	0.93	1.28	58
D_2O	0.51	0.18	21,000
C	0.158	0.056	200

TABLE 1 Slowing Down Properties of Common Moderators

Note that the number density N must not be too small. Helium, for example, has sufficiently large values of ξ and σ_s to be a good moderator but its number density is too *small* to have a significant impact on the energy distribution of neutrons in a reactor. Conversely, for the same reason gases such as helium may be considered as *coolants* for fast reactors since they do not degrade the neutron spectrum appreciably.

The table also includes the slowing down ratio, which is the ratio of the material's slowing down power to its thermal absorption cross section. If the thermal absorption cross section $\sum_a(E_{thermal})$ is large, a material cannot be used as a moderator; even though it may be effective in slowing down neutrons to thermal energy, it will then absorb too many of those same neutrons before they can make collisions with the fuel and cause *fission.* Note that heavy water has by far the largest slowing down ratio, followed by graphite and then by ordinary water. Power reactors fueled by natural uranium can be built using D_2O as the moderator. Because graphite has poorer moderating properties, the design of natural uranium fueled power reactors moderated by graphite is a more difficult undertaking.[13]

2.6.1. Thermal Neutrons

At lower energies, in the thermal neutron range, we again use Eq. (19) as our starting point. The fission term on the right vanishes. The source of neutrons in this case comes from those scattering down from higher energies. We may represent this as a scattering source. We divide the integral in Eq. (19) according to whether E is less than or greater than the *cutoff energy* for the thermal neutron range, typically taken as *Eo=1.0 eV*. We then partition the equation as;

$$\Sigma_t(E)\varphi(E) = \int_0^{E_0} \Sigma_s(E' -> E)\varphi(E')dE' + s(E)q_0 \qquad E < E_0 \qquad 22$$

Where

$$s(E)q_0 = \int_{E_0}^{\infty} \Sigma_s(E' -> E)\varphi(E')dE' \qquad E' > E_0 \qquad 23$$

is just the source of thermal neutrons that arises from neutrons making a collision at energies $E' > Eo$, but having an energy of $E < Eo$ after that collision and q_0 is the slowing down density. The source may be shown to be proportional to the slowing down density at *Eo*. The solution of Eq. (22) would become time dependent, for without absorption in an infinite medium the neutron population would grow continuously with time since each slowed down neutron would go on scattering forever. If after some time the slowing down density were set equal to zero, an equilibrium distribution would be achieved satisfying the equation;

$$\Sigma_s(E)\varphi_M(E) = \int_0^{E_0} \Sigma_s(E' -> E)\varphi_M(E')dE'. \qquad 24$$

One of the great *triumphs* of kinetic theory was the proof that for this equation to be satisfied, the principle of detailed balance must be obeyed. Detailed balance states that;

$$\Sigma_s(E->E')\varphi_M(E) = \Sigma_s(E'->E)\varphi(E'), \quad 25$$

no matter what scattering law is applicable. Equally important, the principle states that in these circumstances the flux that satisfied this condition is the form found by multiplying the famed Maxwell-Boltzmann distribution, given by Eq. (25), by the neutron speed to obtain;

$$\varphi_M(E) = \frac{1}{(kT)^2} E \exp(-E/kT) \quad 26$$

following normalization to;

$$\int_0^\infty \varphi_M(E)dE = 1 \quad 27$$

In reality some absorption is always present. Absorption shifts the thermal neutron spectrum upward in energy from the Maxwell- Boltzmann distribution, since complete equilibrium is never reached before neutron absorption takes place. Figure 2 illustrates the upward shift, called spectral hardening, which increases with the size of the absorption cross section.

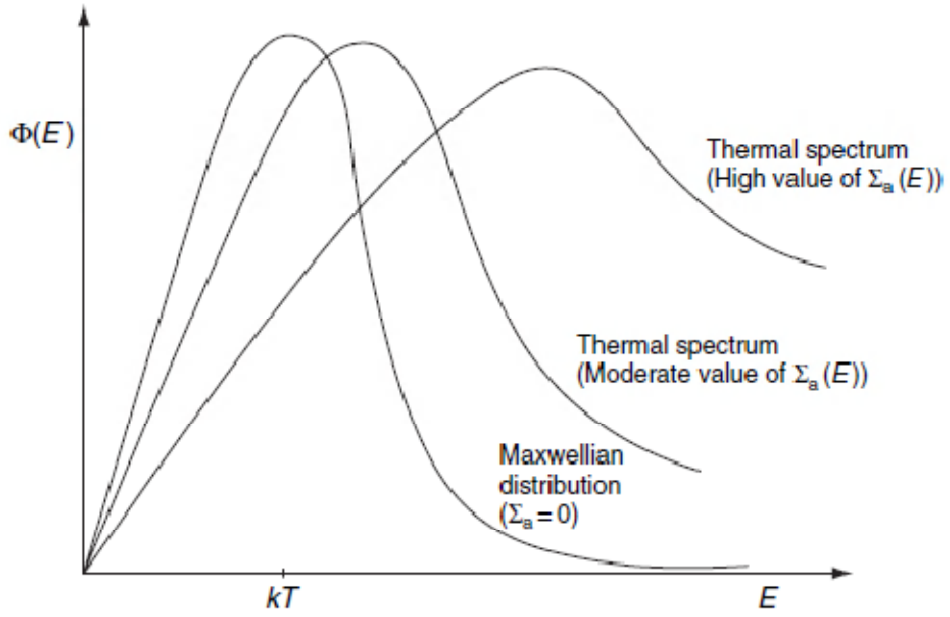

FIGURE 2. Thermal spectra compared to a Maxwell-Boltzmann distribution.[13]

2.6.2. Neutron Lifetime

Two distinct strategies have been employed to measure the neutron lifetime. *The first measurements* were performed using thermal or cold beams of neutrons and measured simultaneously both the average number of neutrons *N* and the rate of neutron decays *dN/dt* from a well-defined fiducial volume in the beam.

The beam technique requires absolute knowledge of the efficiencies to extract the lifetime from $dN/dt = -N/\tau_n$. A significant improvement in the precision was obtained by implementing a segmented proton trap to better define the fiducial volume.

With the advent of UCN (Ultra Cold Neutron) production techniques, *a second approach* to lifetime measurements was developed that confines neutrons in material "bottles" or magnetic fields and measures the number of neutrons remaining as a function of *time*. At a time *t* the number of neutrons is given by $N(t) = N(0)e^{-t/\tau_n}$, so by measuring *N(t)* at different times, one can determine the neutron lifetime (τ_n).[12]

2.7. Neutron Cross Sections

Neutrons are neutral particles. Neither the electrons surrounding a nucleus nor the electric field caused by a positively charged nucleus affect a neutron's flight. Thus neutrons travel in straight lines, deviating from their path only when they actually collide with a *nucleus* to be *scattered* into a new direction or *absorbed.* The life of a neutron thus consists typically of a number of scattering collisions followed by absorption at which time its identity is lost. To a neutron traveling through a solid, space appears to be quite *empty*.

Since an atom has a radius typically of the order of 10^{-8} *cm* and a nucleus only of the order of 10^{-12} *cm*, the fraction of the cross sectional area perpendicular to a neutron's flight path blocked by a single tightly packed layer of atoms would be roughly $(10^{-12})^2/(10^{-8})^2 = 10^{-8}$, a small fraction indeed. Thus neutrons on average penetrate many millions of layers of atoms between collisions with nuclei.

2.7.1. Microscopic and Macroscopic Cross Sections

To examine how neutrons interact with nuclei, we consider a beam of neutrons traveling in the *x* direction as indicated in Fig. 4. If the beam contains n''' neutrons per cm^3 all traveling with a speed '*v*' in the *x* direction, we designate $I = n'''v$ as the *beam intensity*. With the speed measured in *cm/s*, the beam intensity units are *neutrons/*cm^2 */s*. Assume that if a neutron collides with a nucleus it will either be absorbed or be scattered into a different direction. Then only neutrons that have not collided will remain traveling in the *x* direction.

This causes the intensity of the un collided beam to diminish as it penetrates deeper into the material.

Let *I(x)* represent the beam intensity after penetrating *x cm* into the material. In traveling an additional infinitesimal distance *dx*, the fraction of neutrons colliding will be the same as the fraction of the *1-cm*^{2} section perpendicular to the beam direction that is shadowed by nuclei. If dx is small, and the nuclei are randomly placed, then the shadowing of one nucleus by another can be ignored. (Only in the rarely encountered circumstance where neutrons are passing through a single crystal does this assumption break down.) Now assume there are *N nuclei/cm*^{3} of the material; there will then be *N dx per cm*^{2} in the infinitesimal thickness.

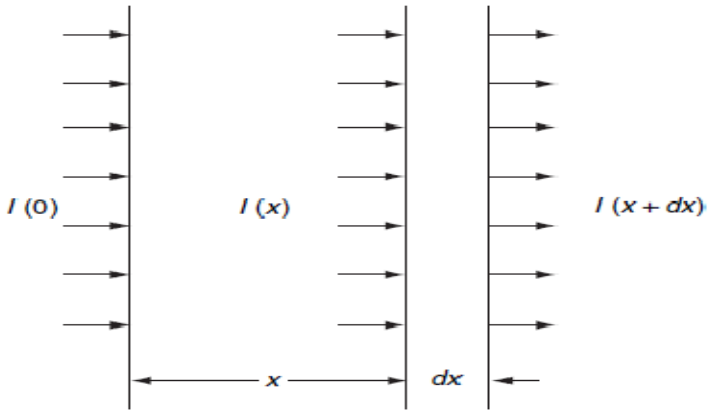

FIGURE 3 Neutron passage through a slab.

If each nucleus has a cross-sectional area of *σ-cm*^{2}, then the fraction of the area blocked is *Nσdx*, and thus we have,

$$I(x+dx) = (1 - N\sigma dx)I(x) \qquad 28$$

Using the definition of the derivative, we obtain the simple differential equation

$$\frac{dI(x)}{dx} = -N\sigma I(x) \qquad 29$$

which may rewritten as

$$\frac{dI(x)}{I(x)} = -N\sigma dx \qquad 30$$

and integrated between *0* and *x* to yield

$$I(x) = I(0)\exp(-N\sigma x) \qquad 31$$

We next define the macroscopic cross section as:

$$\sum = N\sigma \qquad 32$$

[13]

Here σ, is referred to as the effective cross sectional area, frequently called the *microscopic cross section.* It follows:

$\boldsymbol{\sigma}$ = number of neutron collisions per unit time with one nucleus per unit intensity of the incident neutron beam, which has units of cm^2 */nucleus.*

The number of nuclei in a target material *made* of a single element (also called the number density), *n,* is obtained from,

$$n = N_a.\rho/A \qquad 33$$

where A is the atomic mass number, $\rho = A/V$, and N_a, is Avogadro's number.[11]

Since the unit of *N* is nuclei/cm^3, ∑, the macroscopic cross section in Eq. (32) must have units of cm^{-1}. The cross section of a nucleus is very small. Thus instead of measuring microscopic cross sections in cm^2 the unit of the barn is commonly used. One barn, abbreviated as *''b,''* is equal to $10^{-24}cm^2$.

The foregoing equations have a probabilistic interpretation. Since *dI(x)* is the number of neutrons that collide in *dx*, out of a total *of I(x), -dI(x)/I(x)=∑dx*, as given by Eq. (30), must be the probability that a neutron that has survived without colliding until *x,* will collide in the next *dx.* Likewise *I(x)/I(0)=exp(-∑x)* is the fraction of neutrons that have moved through a distance *x* without colliding. If we then ask what is the probability *p(x)dx* that a neutron will make its first collision in *dx,* it is the probability that it has survived to *dx* and that it will collide in *dx*. If its probability of colliding in *dx* is independent of its past history, the required result is obtained simply by multiplying the probabilities together, yielding,

$$P(x)dx = \sum \exp(-\sum x)dx \qquad 34$$

From this we can calculate the mean distance traveled by a neutron between collisions. It is called the *mean free path* and denoted by λ:

$$\lambda = \int_0^\infty xP(x)dx = \int_0^\infty x\Sigma \exp(-\Sigma x)dx = 1/\Sigma . \qquad 35$$

Thus the mean free path is just the *inverse* of the *macroscopic cross section*.[13]

2.7.2. Cross Section Energy Dependence

Let we begin our description of the energy dependence of cross sections with hydrogen; since it consists of a single proton, its cross section is easiest to describe. Hydrogen has only elastic scattering and absorption cross sections. Since it has no internal structure, hydrogen is incapable of scattering neutrons in elastically. Figure 4a is a plot of hydrogen's elastic scattering cross section. The capture cross section, shown in Fig. 4b, is inversely proportional to $\sqrt{E}$, and since energy is proportional to the square of the speed, it is referred to as a *1/v*. Hydrogen's capture cross section which is the same as absorption since there is no fission is only large enough to be of importance in the thermal energy range. The absorption cross section is written as:

$$\sigma_a(E) = \sqrt{\frac{E_0}{E}}\sigma_a(E_0) \qquad 36$$

Conventionally, the energy is evaluated at $Eo = kT$, in combination with the standard room temperature of $T=293.61\ K$. Thus $Eo = 0.0253\ eV$. For most purposes we may ignore the low and high energy tails in the scattering cross section.

a) Elastic scattering

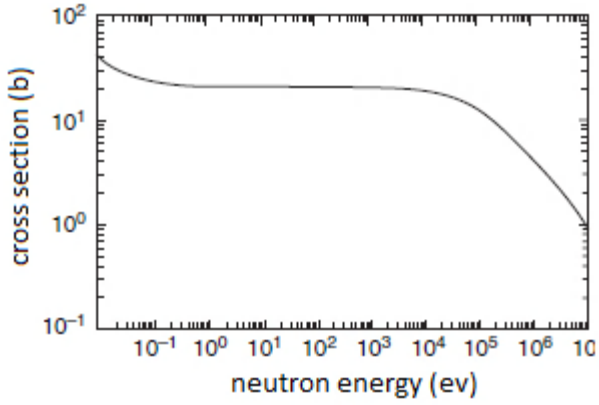

b) Absorption

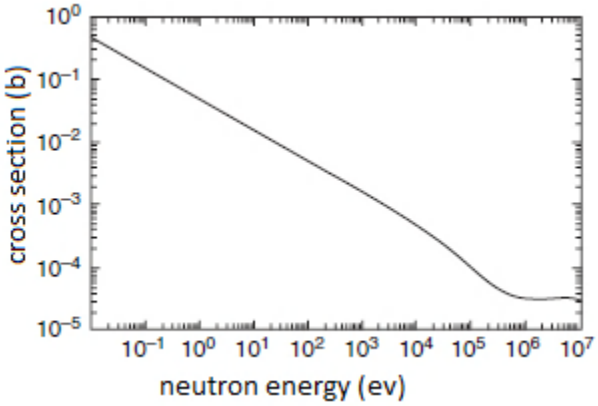

FIGURE 4 Microscopic cross sections of hydrogen-1. (a) Elastic scattering, (b) Absorption.

The total cross section may then be approximated as:

$$\sigma_t(E) = \sigma_s + \sqrt{(E_0/E)}.\ \sigma_a(E_0) \qquad 37$$

Like hydrogen, other nuclei have elastic scattering cross sections, which may be equated to simple billiard ball collisions in which kinetic energy is conserved. These are referred to as *potential scattering cross sections* because the neutron scatters from the surface of the nucleus, rather than entering its interior to form a *compound nucleus*. Potential scattering cross sections are energy *independent* except at very low or high energies. Their magnitude is directly proportional to the cross sectional area of the nucleus, where the radius of the nucleus may be given in terms of the atomic weight as $R=1.25 \times 10^{-13} A^{1/3}$ *cm*. Further understanding of neutron cross sections, however, requires that we examine reactions resulting from the formation of compound nuclei.[13]

2.7.3 .Compound Nucleus Formation

If a neutron enters a nucleus instead of scattering from its surface as in potential scattering a compound nucleus is formed, and it is in an excited state. There are *two* contributions to this excitation energy.

The first derives from the kinetic energy of the neutron. We determine excitation energy as follows. Suppose a neutron of mass *m* and velocity *v* hits a stationary nucleus of atomic weight *A* and forms a compound nucleus. Conservation of momentum requires that;

$$mv = (m + Am)V \tag{38}$$

Kinetic energy, however, is not conserved the formation. The amount lost is:

$$\Delta E_{ke} = \frac{1}{2} mv^2 - \frac{1}{2}(m + Am)V^2 \tag{39}$$

where *V* is the speed of the resulting compound nucleus. Eliminating *V* between these equations then yields,0

$$\Delta E_{ke} = \frac{A}{A+1}\frac{1}{2} mv^2 \tag{40}$$

Which may be shown to be identical to the neutron kinetic energy before the collision measured in the center of mass system. Hence we hereafter denote it by E_{cm}.

The second contribution to the excitation energy is the *binding energy* of the neutron, designated by E_B. The excitation energy of the compound nucleus is $E_{cm} + E_B$. Note that even very slow moving thermal neutrons will excite a nucleus, for even though $E_{cm} << E_B$, the binding energy by itself may amount to a *MeV* or more.

The effects of the excitation energy on neutron cross sections relate strongly to the internal structure of the nucleus. Following formation of a compound nucleus *one of two* things happen: *the neutron may be reemitted,* returning the target nucleus to its ground state; this scattering is elastic, even though a compound nucleus was formed temporarily in the process. Alternately, *the compound nucleus may return to its ground state by emitting one or more gamma rays*; this is a neutron capture reaction through which the target nucleus is transmuted to a new isotope as the result of the neutron gained.

2.7.4. Resonance Cross Sections

The probability of compound nucleus formation greatly increases if the excitation energy brought by the incident neutron corresponds to a quantum state of the resulting nuclei. Scattering and absorption cross sections exhibit resonance peaks at neutron kinetic energies corresponding to those quantum states. Each nuclide has its own unique resonance structure, but generally the heavier a nucleus is, the more energy states it will have, and they will be more closely packed together. The correlation between quantum state density and atomic weight results in the resonance of lighter nuclides beginning to occur only at *higher energies*. For example, the lowest resonance in carbon-12 occurs at *2 MeV*, in oxygen-16 at *400 keV*, in sodium-23 at *3 keV*, and in uranium-238 at *6.6 eV*. Likewise the resonances of lighter nuclei are more widely spaced and tend to have a smaller ratio of capture to scattering cross section. [13]

At thermal energies, the cross section of a reaction is completely determined by the parameters of several low-lying resonances. These parameters, such as the neutron strength function, the mean level spacing, and the average reaction width, vary significantly from one nucleus to another.

The main idea of statistical approach is to account for the random fluctuations of resonance parameters by introducing the universal probability distribution *P(z)*. Here, the quantity $z = \sigma_r/\sigma_r^*$ is the ratio of the actual cross section of the reaction *r* to its "expected" value σ_r^*, the latter being calculated for each nuclide individually through its own average parameters.

The contribution of a single resonance with spin *J*, energy E_i, neutron width Γ_{ni} and the exit channel width Γ_{ri} to the reaction cross section is described by the Breit-Wigner formula as;

$$\sigma_{ri} = \frac{\Pi}{K^2}\frac{2J+1}{2(2I+1)}\frac{\Gamma_{ni} * \Gamma_{ri}}{(E-E_i)^2 + (\frac{\Gamma_i}{2})^2}. \qquad 41$$

Here,

$$K^2 = (\frac{A}{A+1})^2 \frac{2mE}{\hbar^2} \quad 42$$

E=incident neutron energy in the laboratory system, and

A and I=atomic weight of the target nucleus and its spin respectively.

At thermal energy, E = E_T = 0.0253 eV, only the s-resonances contribute to the cross section, i.e., J = I + ½ or J = I – ½ . The inequalities $E_T << E_i$ and $\Gamma_i << E_i$ are usually true, so that Eq. (41) turns into;

$$\sigma_{ri} = \frac{\Pi}{K^2} \frac{2(I \pm 1/2)+1}{2(2I+1)} * \frac{\Gamma_{ni} * \Gamma_{ri}}{E_i^2}. \quad 43$$

To estimate the cross-section value, let us represent it as the sum of the independent resonance contributions under the following simplifying assumptions:

1. All reaction widths are equal to the corresponding mean values (depending on J):

$$\Gamma_{ri} = \overline{\Gamma}_r(J), \Gamma_{ni} = \overline{\Gamma}_n^0(J)(E/E_0)^{1/2}, E_0 = 1eV. \quad 44$$

2. The energy spacing between the resonances with spin J are constant:

$$E_{i+1} - E_i = \overline{D}(J). \quad 45$$

3. The resonances are located symmetrically with respect to the zero neutron energy point:

$$E_i = \overline{D}(J)(I - 1/2). \quad 46$$

Using these assumptions, we come to the following expression for the expected cross-section value σ_r^*;

$$\sigma_r^* = \frac{\Pi}{K^2}(E/E_0)^{1/2}\{\frac{g(J_1)*\overline{\Gamma}_n^0(J_1)*\overline{\Gamma}_r(J_1)}{[\overline{D}(J_1)/2]^2} + \frac{g(J_2)*\overline{\Gamma}_n^0(J_2)*\overline{\Gamma}_r(J_2)}{[\overline{D}(J_2)/2]^2}\} * \sum_{i=-\infty}^{\infty} \frac{1}{(2i-1)^2} \quad 47$$

$\overline{\Gamma}_n^0(J)$ is the mean neutron width, reduced to E_0=1eV, and

$$g(J) = \frac{(2J+1)}{2(2I+1)} \quad 48$$

is the statistical factor.

The value of sum is equal to $\pi^2/4$.

For the neutron capture reaction $\overline{\Gamma}_r(J) = \overline{\Gamma}_\gamma$ there are two systems of resonances (with spins J_1 = I + 1/2 and J_2 = I – 1/2) that give comparable contributions to the cross section.

After substitution of the numerical factors corresponding to the thermal energy of the incident neutron (E = E_T), we obtain;

$$\sigma_\gamma^* = 0.404*10^8(\frac{A+1}{A})^2 * F(I) * \frac{S_0 \overline{\Gamma}_\gamma}{\overline{D}_0} \quad 49$$

Here, $F(I) = g^2(J_1) + g^2(J_2) = \frac{(I+1)^2 + I^2}{(2I+1)^2}$,

$$S_0 = \frac{g\overline{\Gamma}_n^o}{\overline{D}_0} \quad 50$$

Is strength function for s-neutrons,

$\overline{D}_0(I)$ =average spacing between s-resonances of the target nucleus with the spin I, which is connected with $\overline{D}(J)$ by the equality

$$\overline{D}_0(I) = g(J)\overline{D}(J). \quad 51$$

For I=0, eq.(49) is reduced to;

$$\sigma_\gamma^* = 0.404*10^8(\frac{A+1}{A})^2 * \frac{S_0\Gamma_\gamma}{\overline{D}_0} \quad 52$$

In particular, the expected value of the thermal capture cross section is expressed through the strength functions of s-resonances S_0 for neutron and $S_{\gamma 0}$ for photons;

$$\sigma_\gamma^* = 0.404*10^8(\frac{A+1}{A})^2 * S_0 * S_{\gamma 0}. \quad 53$$

Where $S_{\gamma 0} = \frac{\Gamma_\gamma}{\overline{D}_0}$ 54

[15, 16]

According to the extreme compound, or black, nucleus model the strength function is constant for all nuclei, and for s-wave neutrons is given by;

$$\frac{\overline{\Gamma_n^0}}{D_0} = \frac{2k_0}{\pi K} = 1*10^{-4} \quad 55$$

Where, *ko* is the wave number for a 1 eV neutron while *K* is the wave number inside the nucleus. [17]

2.8. Radiation detectors

There are radiation detectors for different types of nuclear reaction which falls into two categories: *gross counters* and *energy sensitive*. Gross counters count each event (gamma or neutron) emission the same regardless of energy. Energy sensitive detectors used in radio-isotope identification devices (RIIDs) analyze a radioactive isotopes distinct gamma energy emissions and attempt to identify the source of the radiation. The detectors are named based on; collection of charge produced by particles due to ionization energy loss (primary ionization), multiplication of primary charges, light collection produced by radiations and recording the actual path of ion traveling in the medium as ionization chamber, scintillation chamber, semiconductor detector, etc.[18]

2.8.1. Scintillation Detectors NaI (Tl)

A scintillation radioactivity detector consists of a *scintillator* or *phosphoc* optically coupled to a photomultiplier tube. The most common scintillator for γ-ray measurements is a large crystal of *NaI* activated with 0.1 to 0.2% *Tl*. The γ-photon is reacting with the detector, ejecting electrons. These electrons produce excitation or ionization in the scintillator crystal. De-excitation of the scintillator occurs via fluorescence in about 0.2 ps by the *Tl+* activator (visible light). The small percentage of *Tl*, the "activator", is added to *shift the wavelength* of the emitted light by the detector to longer wavelength for two reasons:

- In order to reduce the *self-absorption* of the emitted de-excitation light by the *NaI* crystal; and
- The shift from *UV* light to visible light increases the sensitivity of the photomultiplier to the emitted light.

The most popular size for routine γ -ray spectrum measurements is a 7.5-cm diameter, 7.5-cm high cylinder. It requires approximately 30 *eV* of energy deposited in *NaI* crystal to produce one light photon. [19]

2.8.2. Solid- State Ionization Detector

The simplest idea for measurement of radioactive decay is by the use of the main property of the *emitted particles* or *photons*. When an ionizing radiation is striking a non conducting or semiconducting material, it forms in it *electrons* and *holes* or *cat ions*. The amount of electrons formed is proportional to the energy of charged particles. The larger number of electrons reduces *the statistical fluctuation* in the number of electrons and hence reduces the width of the radiation signal in the detector (measured as FWHM = full width at half maximum of the peak).

The *smaller* FWHM leads to *much higher resolution*. The voltage pulse produced at the output of the *preamplifier* is proportional to collected charge and independent of detector capacitance. However, the output pulse from the preamplifier is too low for sorting by the multichannel analyzer (MCA). Further amplification is done by the main *amplifier*, serves to *shape the pulse*. In order to reduce the noise due to the leakage current of the electrons in the conduction band agitated by thermal excitation, the semiconductor crystal is cooled to nitrogen temperature.

Of all semiconductor materials, germanium is exclusively used for modern γ-ray spectrometry since only for Ge and Si can adequately pure material be prepared. Si is suitable only for X-ray measurements, due to its *low atomic number*, which reduces the interaction cross-section. In the mid *1970s*, advances in germanium purification technology made available high-purity germanium that could be used for γ -ray spectrometry detection without lithium drifting. These intrinsic germanium detectors are usually called *HPGe* (abbreviation for high-purity germanium). *HPGe* and *Ge(Li)* detectors are virtually identical from the point of view of measurement. However, due to the more convenient use of *HPGe*, they completely replace *Ge(Li)* detectors in contemporary γ-ray spectroscopy.[19]

2.8.3. High Purity Germanium detector (HPGe)

HPGe detectors are made by highly refining the element germanium and growing it into a crystal. The crystal goes through a series of processing steps culminating in the attachment of positive and negative contacts which turn it into an electronic diode. The special property of this diode is that *it conducts current in proportion to the energy of a photon (gamma ray) depositing energy in it.* [18]

HPGe provides positive identifications

Due to its far superior resolution, *HPGe* is the only radiation detection technology that provides sufficient information to accurately and reliably identify radionuclide's from their passive gamma ray emissions. *HPGe* detectors have 20-30 times better resolution than *NaI* detectors. Also, unlike *NaI* detectors, *HPGe* detectors are resistant to information (signal) degradation caused by changes in background radiation, shielding, multiple radionuclide interference, and temperature variations.

HPGe is also much more effective than *NaI* and Cadmium Zinc Telluride (CZT) detectors in stand-off radionuclide identifications such as are encountered in vehicle or shipping container inspections. [18]

2.8.4. HPGe detector versus NaI and CZT detectors in distinguishing dangerous nuclear material

The figure below (Figure 5) is a comparison of three "fingerprints" of the two types of radioactive material (plutonium and iodine) captured using a *low resolution NaI* detector (Blue), a *medium resolution* detector *CZT* (Black), and a *high resolution HPGe* detector (Red). The "peaks" in these graphs represent the unique fingerprints of the two radioactive materials.

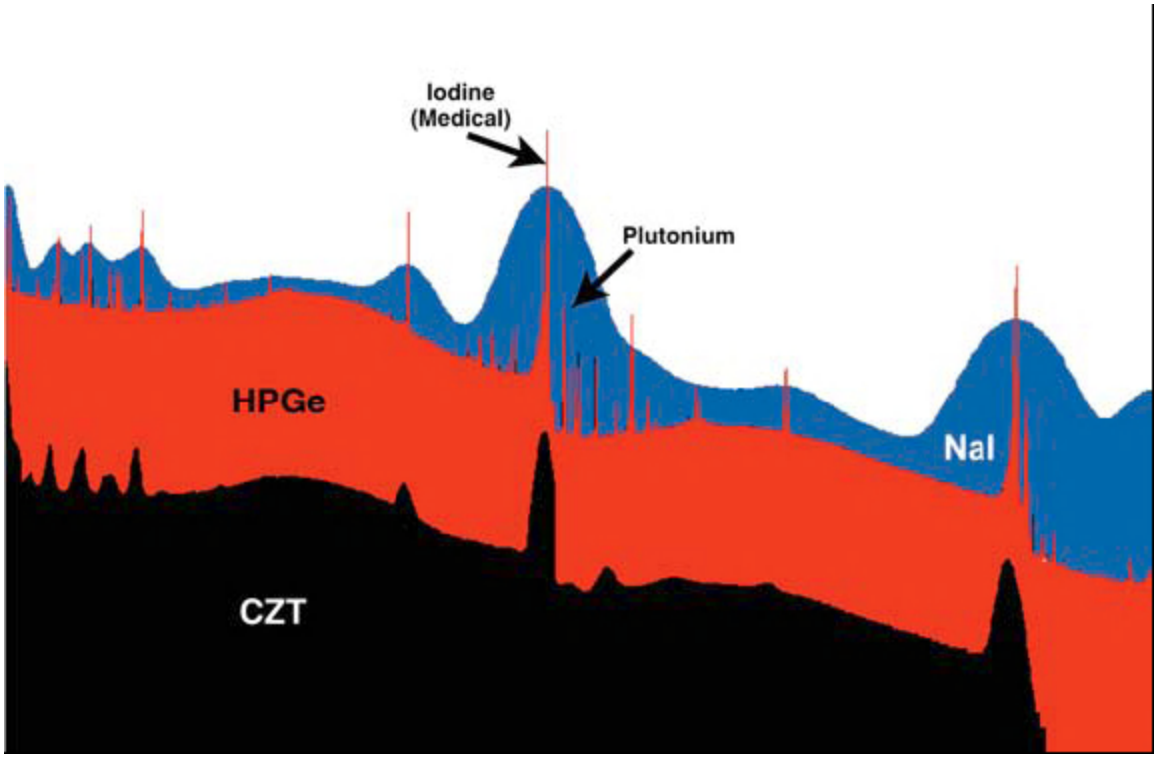

FIGURE.5: Radioactive Material Fingerprints of Same Material Viewed with Three Types of Technology.

The characteristic peaks (or fingerprints) from iodine and plutonium are very close to one another. However, in the blue *(NaI)* and black *(CZT)* graphs, they appear as one peak, whereas in the red graph *(HPGe)* the peaks are clearly distinguishable. The *NaI* and *CZT* systems are unable to find the dangerous nuclear material (plutonium)[19]

The narrower the peak (lower FWHM), the better is the ability of the *detector* to separate two close peaks, i.e., better *resolution*.

The relative efficiency decreases with increasing energy due to the higher *Z* of iodine compared to germanium. For most applications, the resolution is more important than efficiency and *Ge* detectors are the more commonly used detectors.[19]

Chapter Three

Experimental Measurements of Thermal Neutron Capture Cross Section

3.1 Objective of the experiment

When a sample of an element irradiated with thermal neutrons it produces an induced activity or emits gamma rays. Prompt and delayed gamma rays are the two types of gammas seen in the induced reaction and beta particles also, from fig (1). Gamma rays and beta particles following capture of neutron and the formation of a compound nucleus are characteristics of that nucleus, and their identification can lead to identification of the presence of a particular element in the sample. In this experiment, two measurements at *ground state* cross section will be done by irradiating the two stable Bromine isotopes (Br-79 and Br-81) by using HPGe detector and beta counter and Meta stable state cross sections are used from reference for the comparison of theoretical calculation and experimental results. Some gammas are unable to seen by HPGe detectors in particular laboratory used for this experiment, which is very small percentage gamma abundance, as well as short life time (ns or ps). To measure the cross section of such elements, beta counters are advised to use. The gamma abundance that comes from Br-80 is very small that, beta counter is used to determine the thermal neutron cross section; while for Br-82 gamma ray comes for long time and cross section will be measured by using HPGe detector.

3.2) Sampling and Modes of Irradiation

The samples prepared for this experiment is compounds of potassium that is two potassium iodides of different masses and potassium bromide. Out of these samples potassium bromide is the subject of interest which was borrowed from India by Prof. A.K Chaubey in a small size sugar like crystal. Due to the volatility of pure iodine atom, the metal iodide salt is preferred for the determination of neutron flux. 99.9 percent of the salt has I-127 than the rest isotopes of iodine. The samples has to be prepared suitably for irradiation in solid form by putting them in the ring of radius 0.55cm and fasting both side by sticky tape, so that, we can have three samples having the following masses.

1, Potassium iodide (sample1) = 0.1985g

2, potassium iodide (sample 2) = 0.6192g

3, potassium bromide = 0.1739g

These masses are measured by using laboratory balance where even air influence is neglected. A sample of interest is sandwiched by two standards these are; two potassium iodides in order to

have fixed geometry. One standard placed in the front of the sample; the one with low mass and the other is placed at the back of the sample. In the irradiation room, the sample is exposed to the neutron where the low mass standard is toward the source by using plexiglas rod, used to place in the neutron source. The disturbance of neutron flux at the center of the source due to the rod is negligible. These samples are irradiated for a needed time based on the half life of gamma and beta emitted from the radioactive nucleus of interest formed when the sample get neutron from the neutron source. In irradiation process, the sample must get a perpendicular neutron source to have a maximum flux. If the sample is tilted by certain angle, neutron flux is reduced and this thermal neutron source is the main needed material in this experiment.

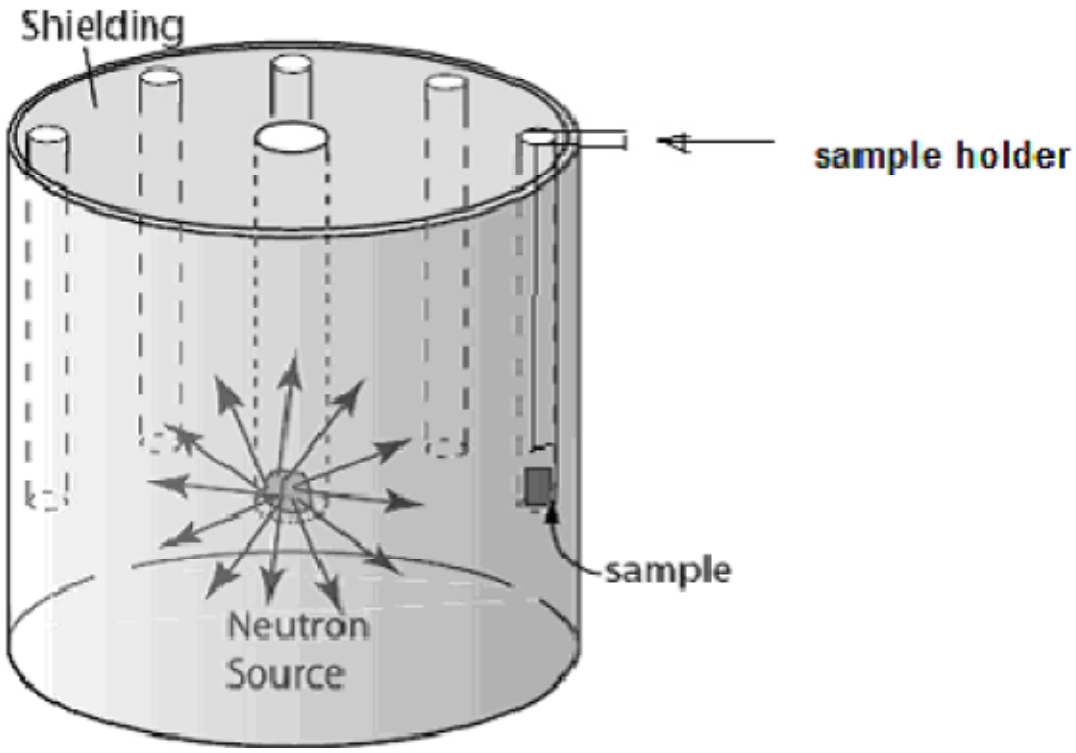

Fig. 6: Am-Be neutron source and sample placement [9]

3.3) Gamma counting

The powerful detector used to count gamma in this experiment is High Purity Germanium detector. This detector is more powerful in gamma detecting than other solid state detectors as discussed in section 2.8.4.

3.3.1) *Apparatus and Flow chart*

After the sample is removed from the neutron source different materials were used to count gammas of several energy including gamma from the back ground. To list them;

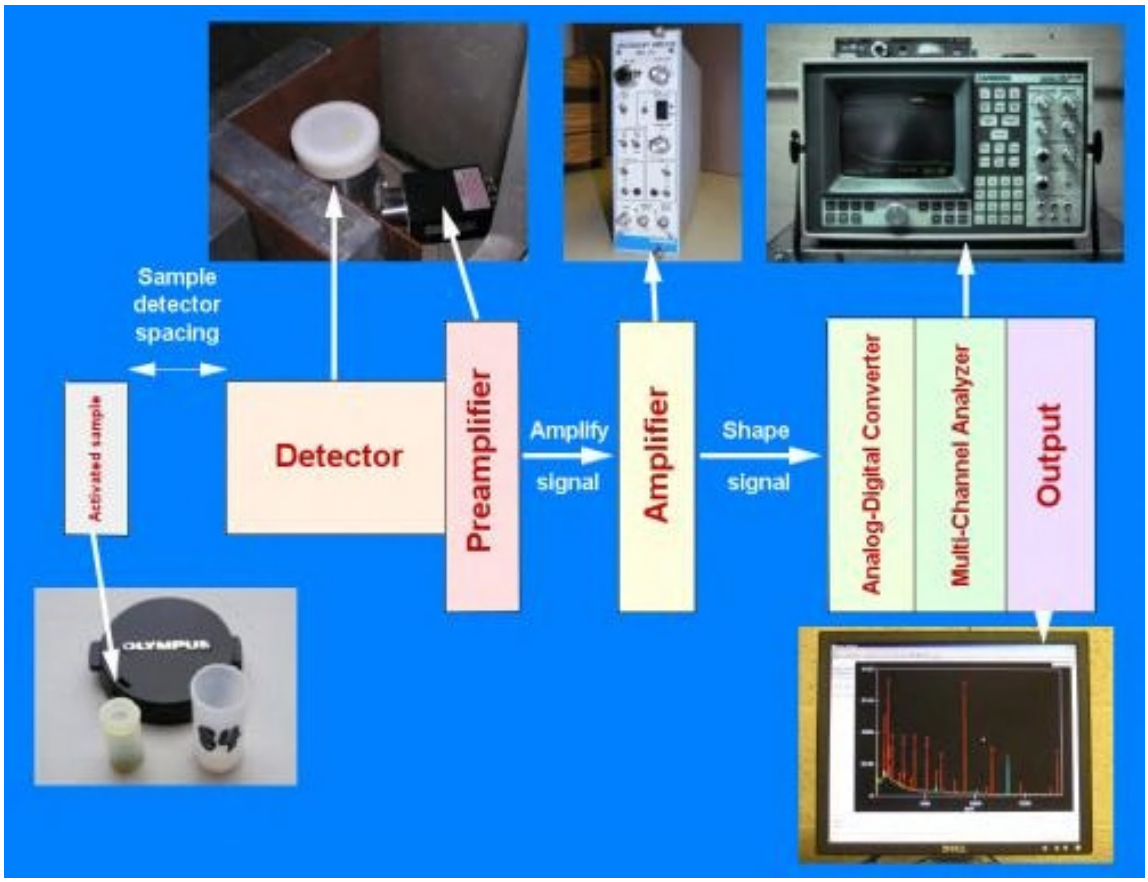

- Liquid nitrogen (77K), Power supplies and different connecting wires are also part of this experiment.

Fig.7 Flow chart for a gamma-ray spectroscopy system [8]

3.3.2) ***Set up in Gamma counting***

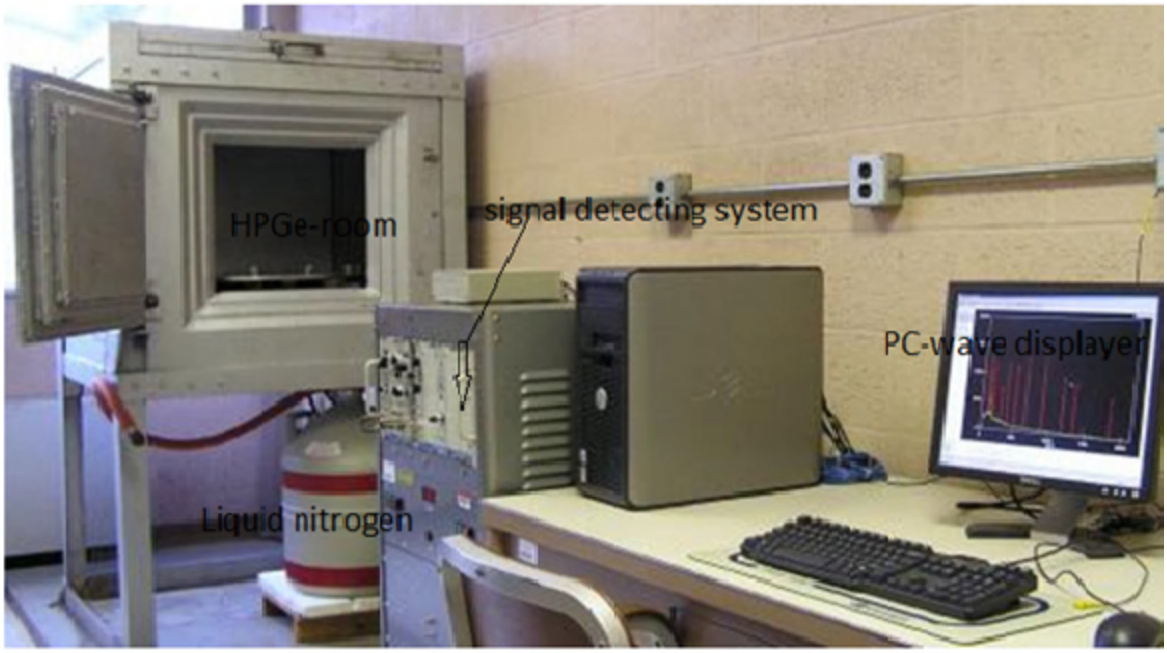

Fig.8 Gamma-ray spectroscopy system [8]

3.3.3) ***Gamma counting procedure***

After samples were brought to detector, it was placed on detector at zero distance at the center of detector by cleaning any other impurities from detector and covered by lead to minimize back ground radiation. The detector detects any gamma comes from sample by its own procedure at very low temperature in a pulse form and sends to multi channel analyzer through pre-amplifier, amplifier and other circuits. The display of multi channel analyzer is seen on the desk top of connected computer in a wave form for a pre sated counting time as in fig.8. In a same procedure three samples were measured alternatively until the decay of samples is observed.

After display is seen areas of needed photo peak is measured and divided to its count time (time needed to see this photo peak) to see activity of an element. As successive measurement for single photo peak is taken, decay of an element is seen.

3.3.4) *Efficiency curve of the HPGe detector*

This curve gives efficiencies of all energies of gamma detected by HPGe which emitted from the radioactive elements at zero distance from the detector which was measured by using Europium source.

Energy of gamma ray	Geometric eff. Of detector
122.8	0.123
244.7	0.086
344.3	0.081
444.0	0.052
778.9	0.035
867.4	0.032
964.0	0.031
1085.8	0.038
1112.1	0.035
1408.1	0.03

Table.2. Decay table of efficiency

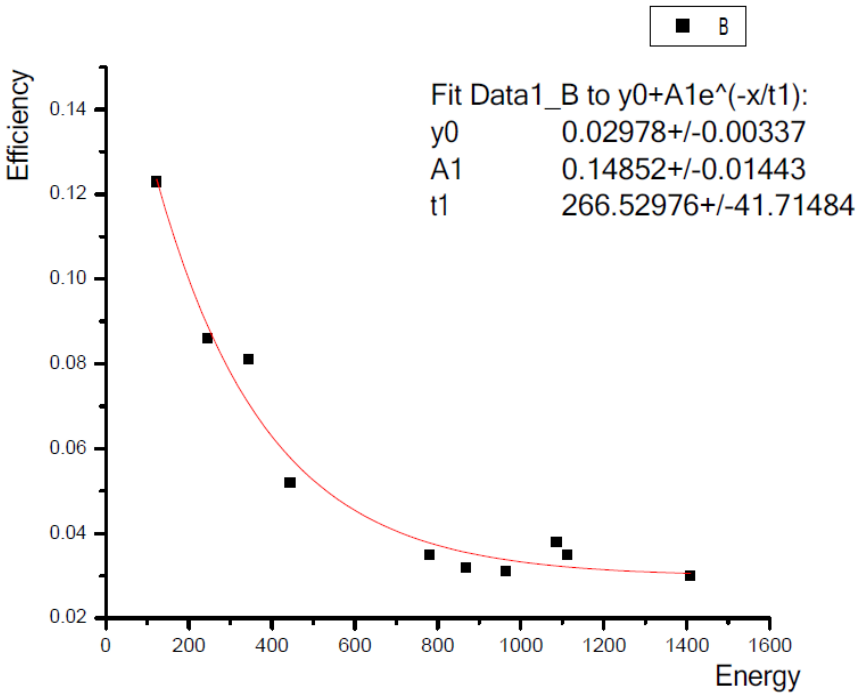

Graph.1 Exponential Decay curve of Efficiency

Before the measurement has taken, calibration of the detector was done by Europium source such that the HPGe detector works properly.

Channel number	Gamma energy
244	121.8
1564	780.4
1966	966.1
2180	1087.9
2232	1113.9
2828	1411.4

Table.3 Calibration Data

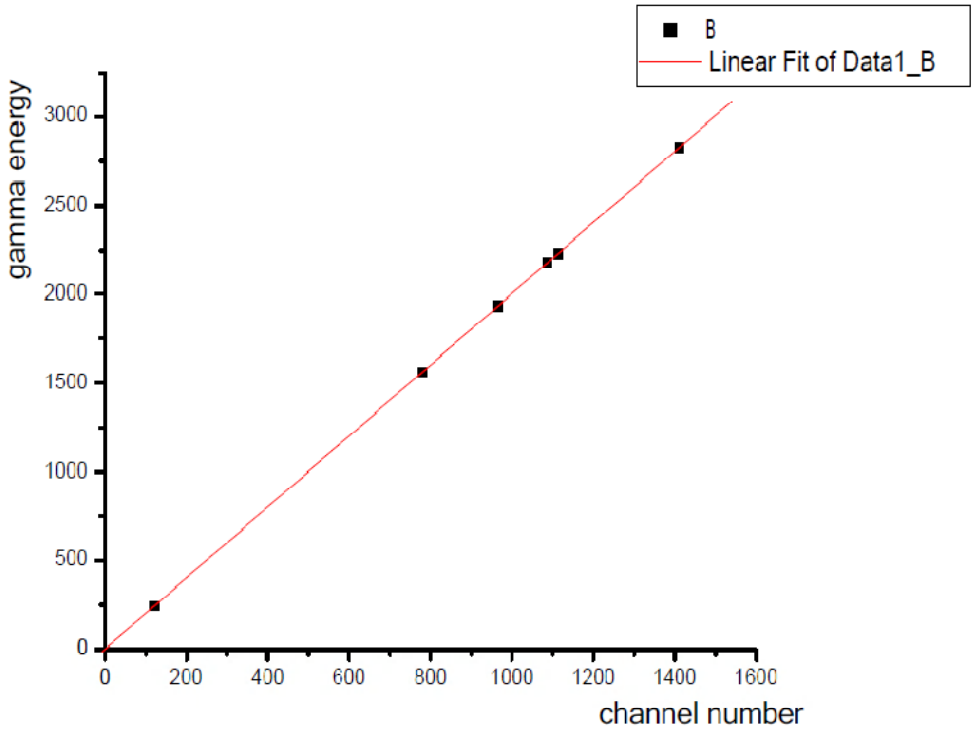

Graph.2 Calibration of detector

3.3.5) ***Measurements of gamma spectrum***

After irradiation stops (after 12-days) the samples was taken by noting down the time of irradiation stopped and taken to the detector as fast as possible in order to minimize the decay time (t_2). The activity of each samples measured consecutively by putting at zero distance from the HPGe detector such that calculation of efficiency is possible from above graph, by changing the counting time (t_3) for a long period of time, until decay of sample seen sufficiently. In measurement the photo peak area was noted and divided by count time to obtain activity. In this part of experiment, the irradiation time is so long that gamma energies of long half life would be expected ($35.34h_r$). This long half life is belongs to Br-82 which is an induced radioactive. So the cross section of Br-82 with half life of $35.34h_r$ is going to measured which is expected to be 0.26 barn.[20]

3.3.6) ***Data and Data Analysis***

No.	Decay time(sec)	Area/count time,with perc.Error
1	435	0.45 ± 7.61%
2	1007	0.27 ± 4.01%
3	1780	0.16 ± 8.56%
4	2850	0.11 ± 1.01%
5	4372	0.055 ± 3.4%
6	6234	0.03 ± 2.1%

Table.4 Decay table of front I target

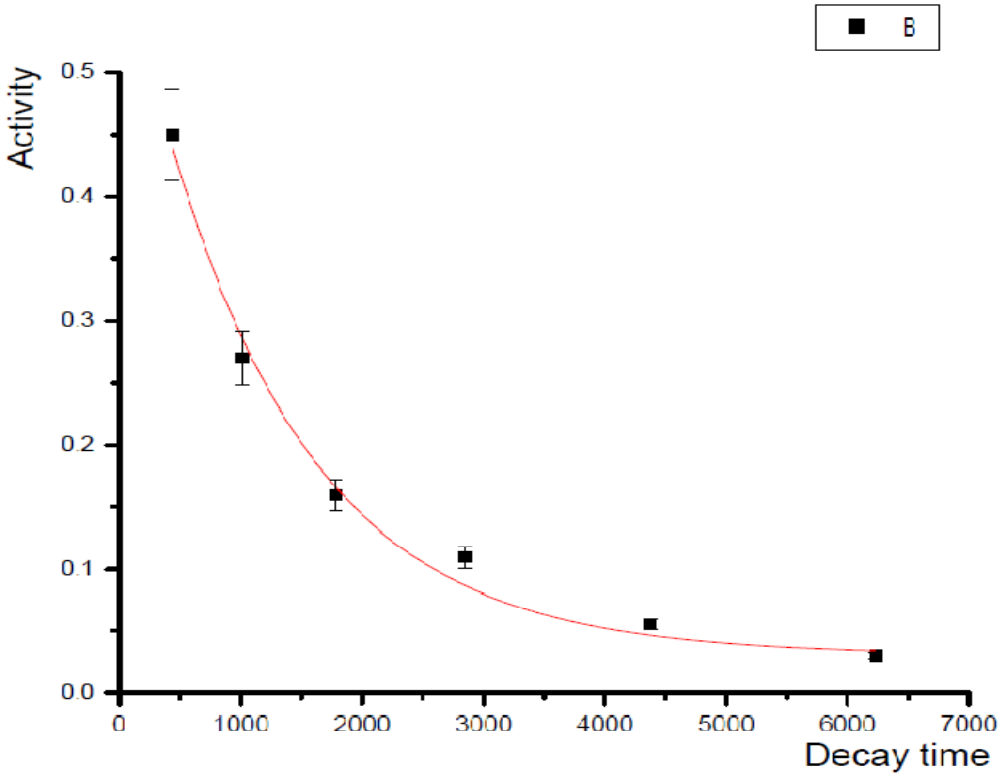

Graph.3 Exponential decay curve of front I target

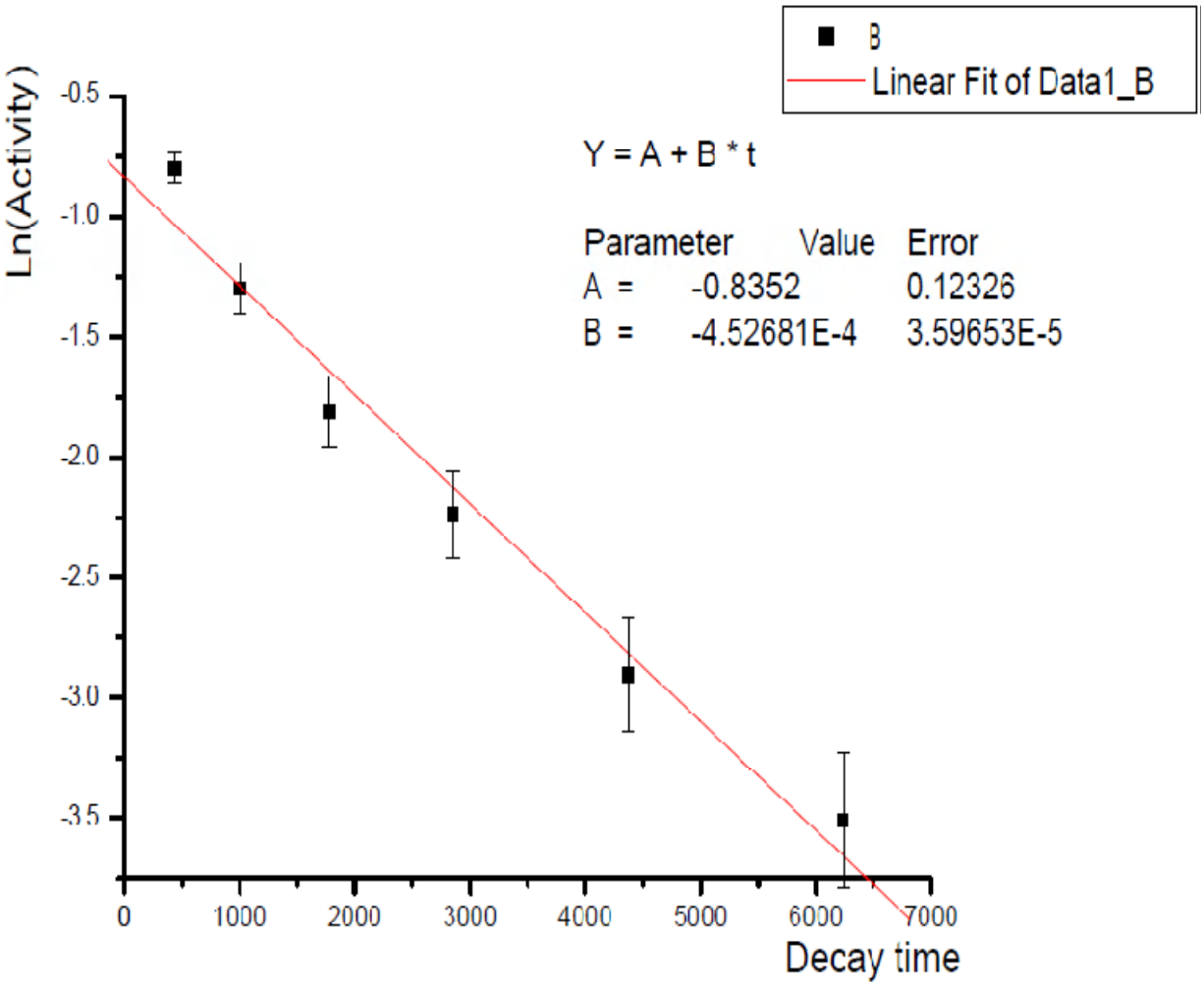

Graph.4 Logarithmic decay curve of front I target

No.	Decay time(sec)	Area/count time with perc.Error
1	639	$0.6 \pm 9.8\%$
2	1224	$0.41 \pm 8.77\%$
3	2047	$0.35 \pm 9.06\%$
4	2924	$0.22 \pm 7.76\%$
5	4880	$0.077 \pm 2.42\%$
6	6992	$0.026 \pm 1.77\%$

Table.5 Decay table of back I target

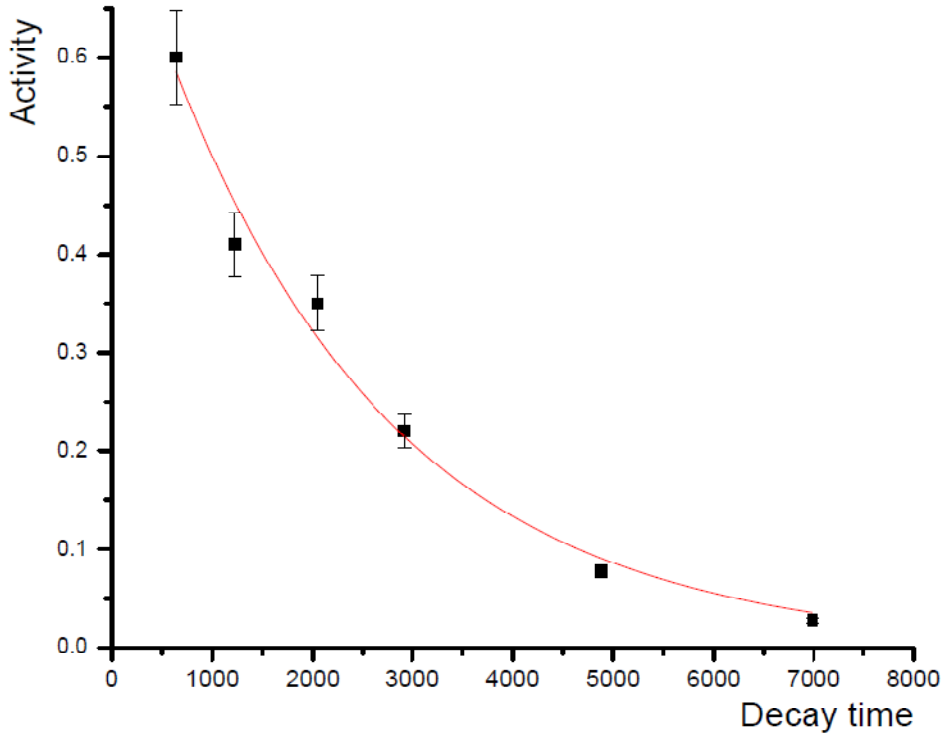

Graph.5 Exponential decay curve of back I target

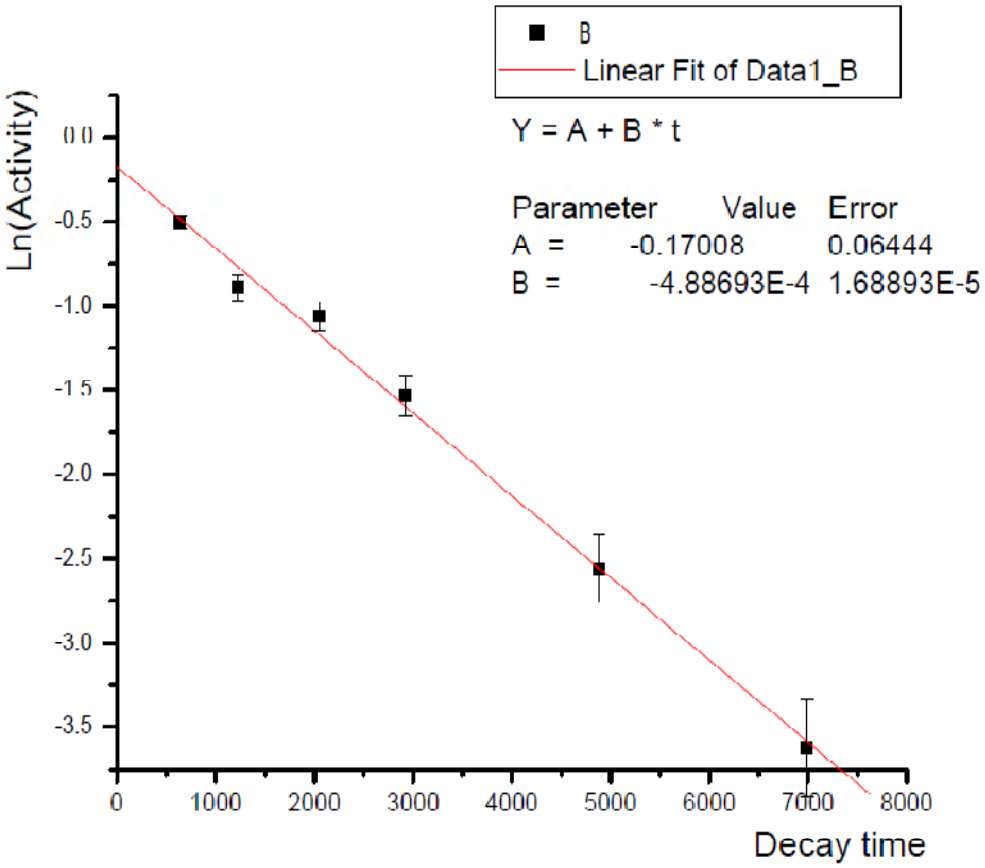

Graph.6 Logarithmic decay curve of back I target

No.	Decay time	Area/count time with perc.Error
1	231	0.30±11.08%
2	1492	0.29±2.25%
3	2310	0.27±2.12%
4	3905	0.28±3.12%
5	5547	0.26±1.10%
6	7801	0.25±11.2%
7	10657	0.26±4.14%
8	15952	0.235±7.31%
9	83759	0.176±6.29%

Table.6 Decay table of Br-82

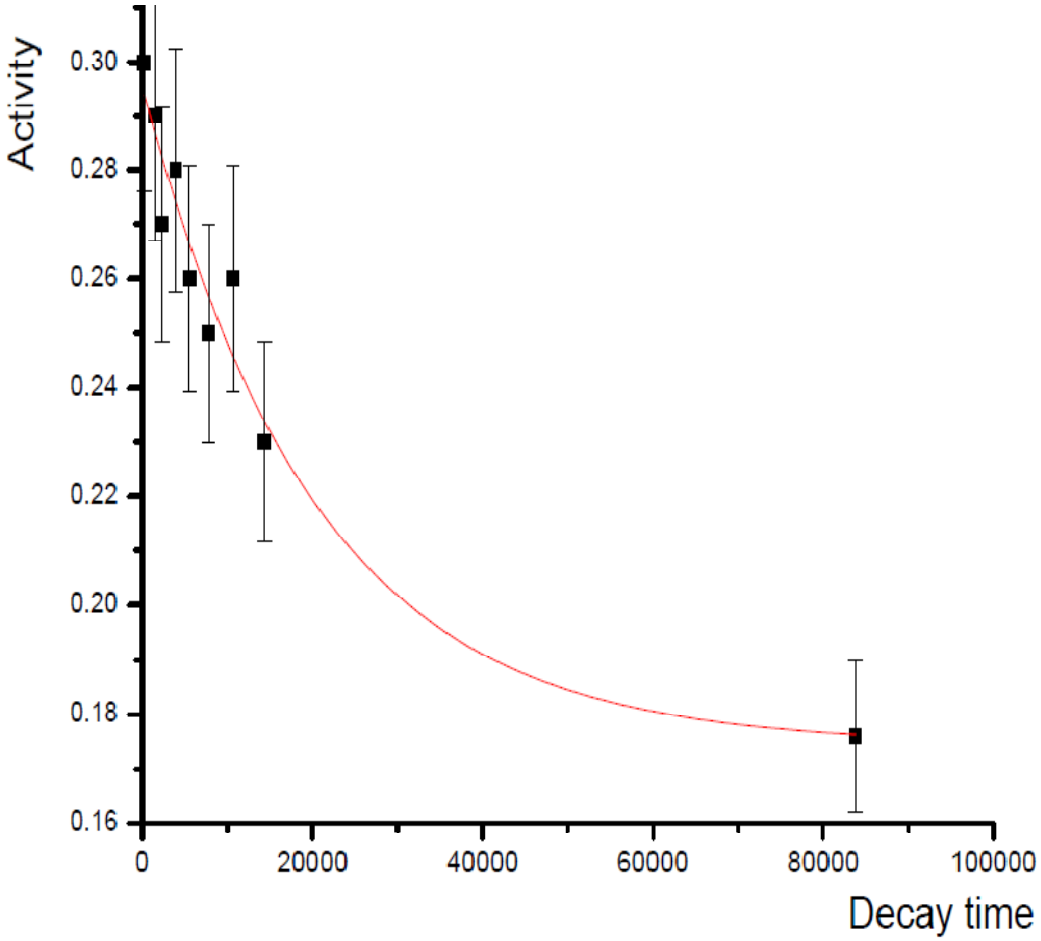

Graph.7 Exponential decay curve of Br-82

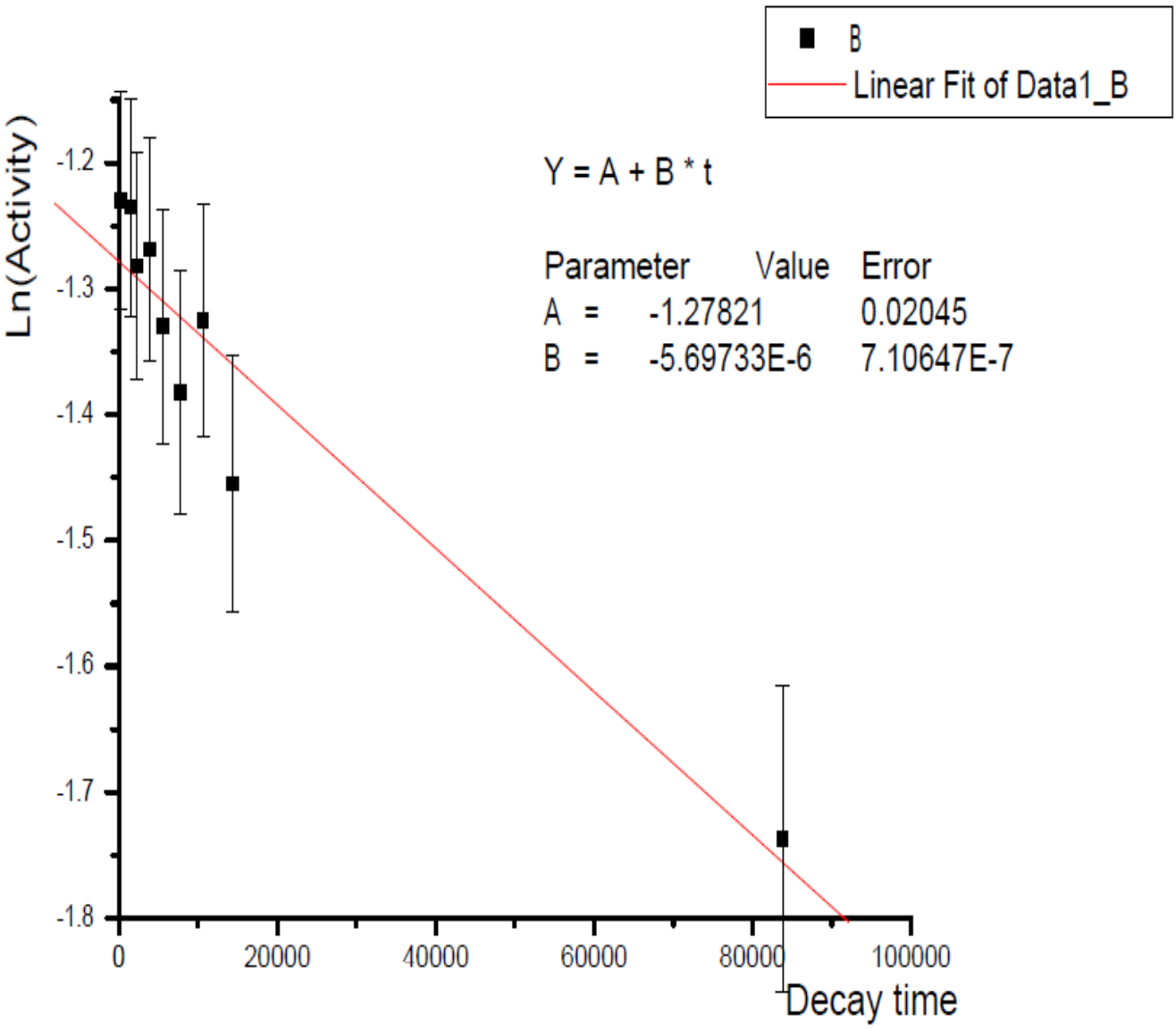

Graph.8 logarithmic Decay curve of Br-82

3.3.7) ***Results and Discussion***

The flux of target sample is now easy to calculate by using the above graphs where the gamma abundance and efficiency of iodine-128 and bromine-82 are given as table below.

	Energy (keV)	Efficiency	Percentage gamma abundance
Iodine	443	0.038	17
Bromine	776	0.058	84

Table.7 parameters used in calculation [20]

The decay constants of two iodine's of different masses are obtained from the graph *Ln(A)* and *t*, that is for the front iodine the graph of logarithm of activity versus time is fitted by the equation Y=A+B*t where B indicates the decay constant λ, such that $\lambda=4.53*10^{-4}$ per second. In the same way for the back iodine the decay constant is given from the graph $\lambda=4.88*10^{-4}$ per second. The decay constant of the front and back iodine is exactly not the same, because of the measurement errors. In average decay constant of iodine; $\lambda=4.7*10^{-4}$ per second. In the calculation we use theoretical decay constant of iodine since its half life is known ($\lambda=4.63*10^{-4}$per sec).

By using this information thermal neutron flux is calculated by rearranging eq. [5] and considering photo peak nature of front iodine;

$$\phi = \frac{(dn/dt)\exp(\lambda t_2)}{N_0 \sigma \varepsilon_G \theta k (1-\exp(-\lambda t_1))(1-\exp(-\lambda t_3))} \qquad 56$$

Where N_{01} is calculated as in eq. [6];

$$N_{o1} = \frac{127g/mole * 0.1985g}{168g/mole} * \frac{6.023*10^{23} atoms/mole}{127g/mole} = 7.12*10^{20} \text{atoms}$$

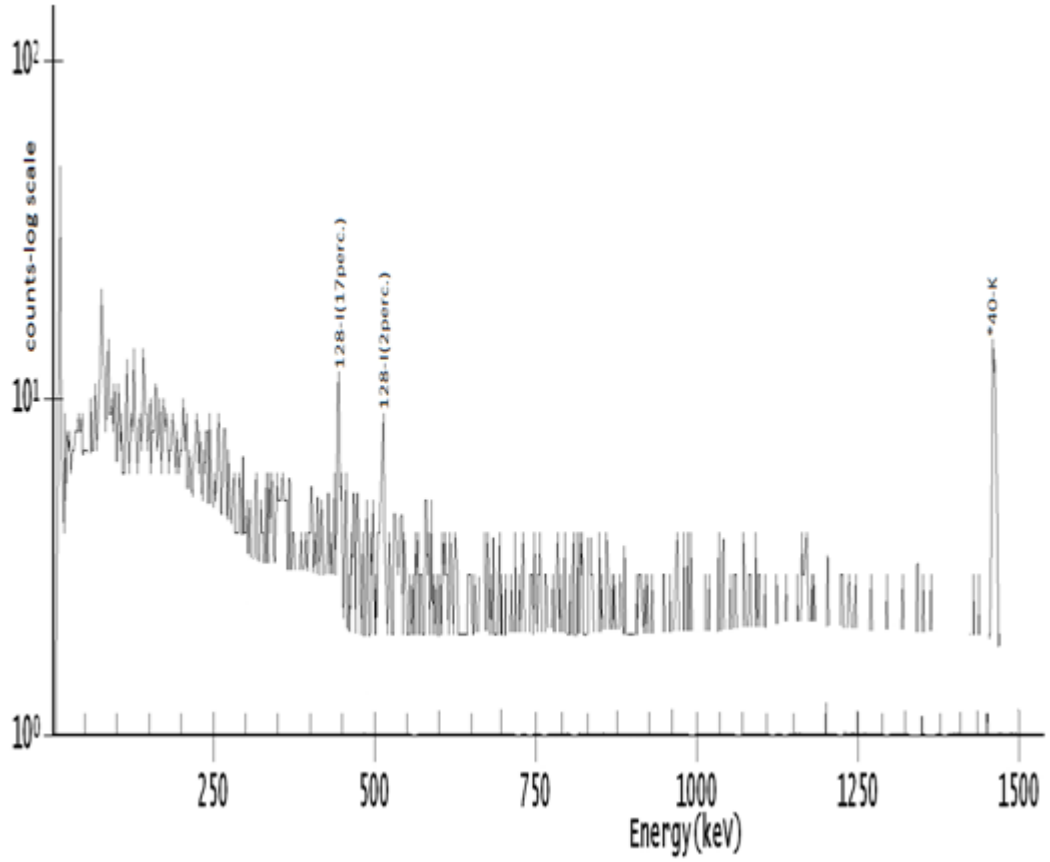

Graph.9 Gamma spectrum with front KI

dn/dt =0.16 dps from table 1, σ=6.2barn and k is calculated by the relation

$$k = \frac{e^{-\mu_m H}}{\mu_m H} = 0.9996 \approx 1 \qquad 57$$

where μ_m is mass absorption coefficient.

$$H = 1/2\ X_m, \qquad 58$$

X_m=ratio of mass of the sample to area of the sample holder.

$1-\exp(-\lambda t_1)=0.997\approx 1$ because t_1 is long as compared to half life of iodine.

Values of t_2 and t_3 are included for the given particular activity in calculation. So thermal neutron flux by front iodine is calculated as;

$$\phi_1 = \frac{0.16 dps}{7.12*10^{20} atoms * 6.2*10^{-24} cm^2 * 0.058 * 0.17} * \frac{e^{(4.63*10^{-4}*1680)}}{(1-e^{-(4.63*10^{-4}*200)})} = 8.3*10^4 \text{n/cm}^2\text{sec}$$

In the same way by using the back iodine number of atoms N_{02} is calculated as;

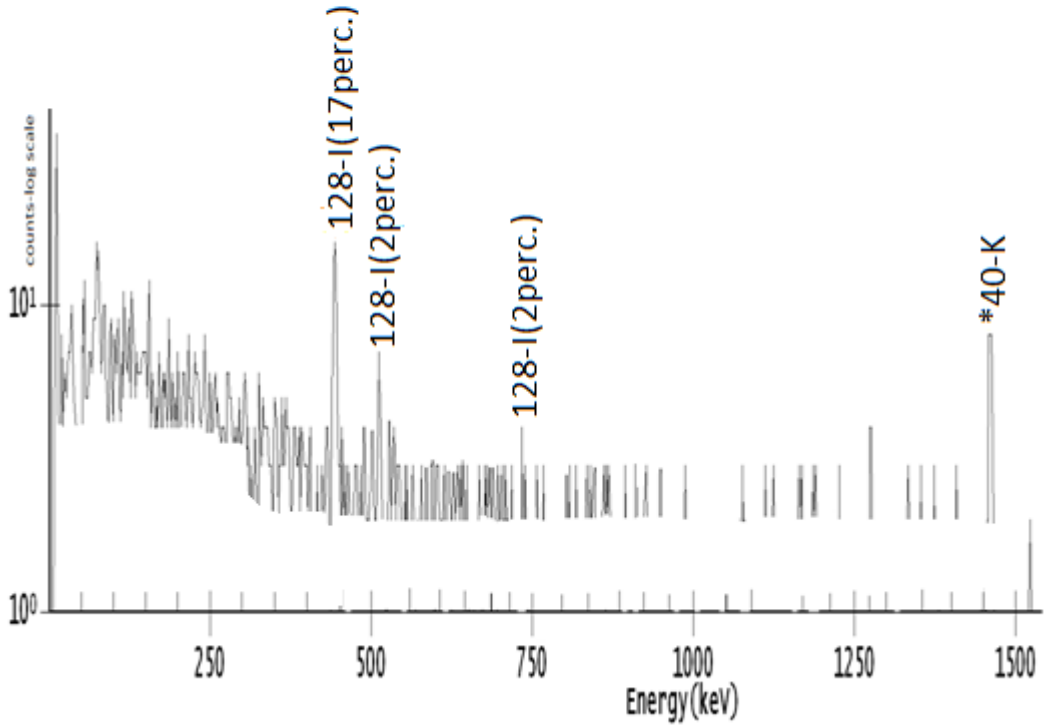

Graph.10 Gamma spectrum with back KI

$$N_{o2} = \frac{127g/mole * 0.6192g}{168g/mole} * \frac{6.023*10^{23} atoms/mole}{127g/mole} = 2.22*10^{21} \text{atoms}$$

dn/dt=0.35dps

K=0.9999967≈1

$$\phi_2 = \frac{0.35dps}{2.22*10^{21} atoms * 6.2*10^{-24} cm^2 * 0.058 * 0.17} * \frac{e^{(4.63*10^{-4}*1947)}}{(1-e^{-(4.63*10^{-4}*200)})} = 7.2*10^4 \text{n/cm}^2\text{sec}$$

The average neutron flux of the two iodine samples calculated as;

$$\Phi = \frac{\phi_1 + \phi_2}{2} = 7.75*10^4 \text{n/cm}^2\text{sec}$$

3.3.8) ***Neutron Capture Cross-Section in Br-81***

To evaluate the capture cross-section of Br-81 by thermal neutron flux already determined, we have to use equation [5], i.e.

$$\sigma = \frac{(dn/dt)\exp(\lambda t_2)}{N_0 \Phi \varepsilon_G \theta k (1-\exp(-\lambda t_1))(1-\exp(-\lambda t_3))}$$

Calculation of thermal cross section is the same as that of flux calculation except the exchange of σ and ϕ.

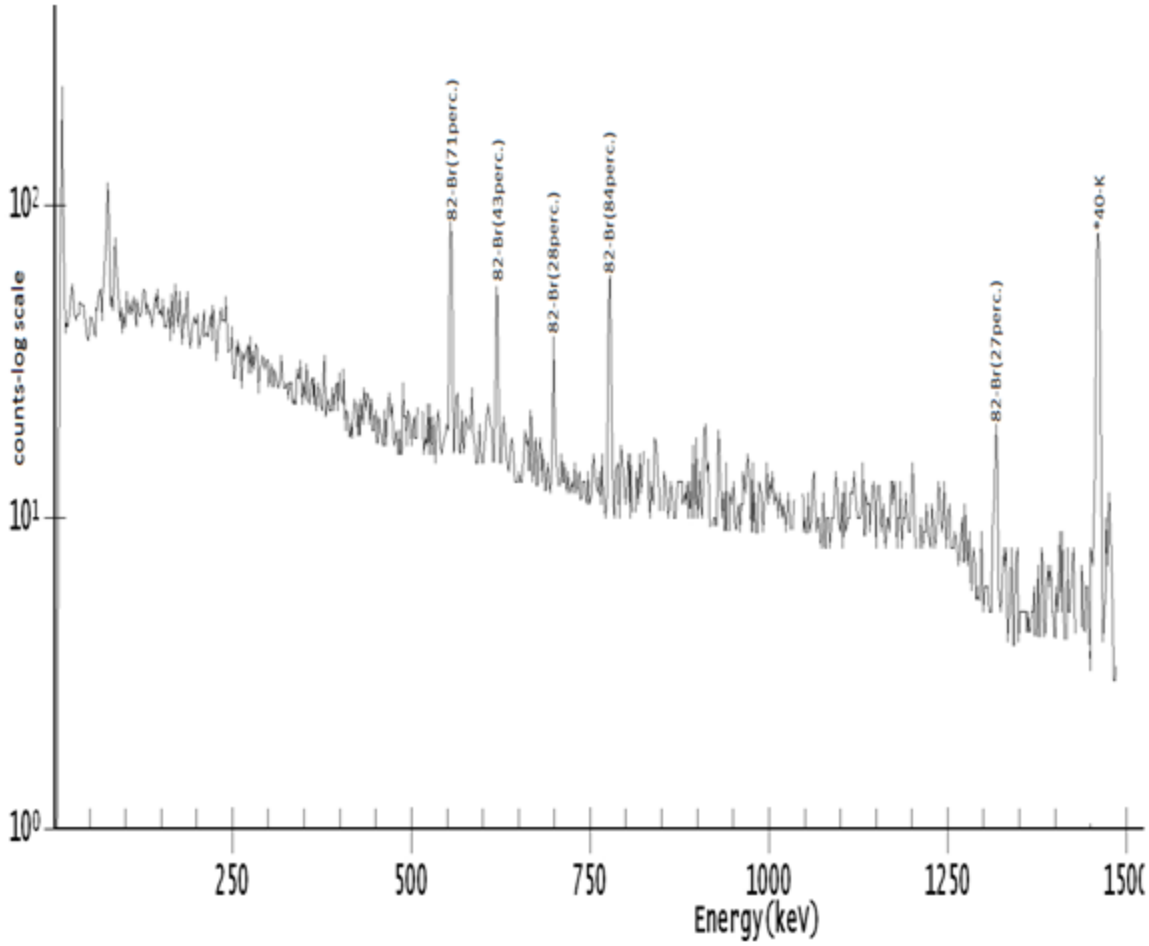

Graph.11 Gamma spectrum with KBr_2

$$N_3 = \frac{81g/mole * 0.1739g}{122g/mole} * 0.4931 \frac{6.023*10^{23} atoms/mole}{81g/mole}$$

$=4.2*10^{20}$atoms

dn/dt is calculated from the above graph[8] at $t_2=0$, where the graph cuts *Ln(Activity)* such that $dn/dt=e^{-1.287}=0.276dps$.

At $t_2=0$ t_1 survive and it gives $(1-e^{-\lambda t_1})\approx 1$, and $t_3=100$sec. Here in 100sec decay of Br-82 is not much seen, since its half life is in days ($35.34h_r$) and ignored from calculation. Efficiency and gamma abundances are given in table [7], *k* by eq. [57], k=0.999995≈1.

$$\sigma = \frac{0.276dps}{4.2*10^{20}*7.75*10^{4}\,n/cm^2\,\text{sec}*0.84*0.038}$$

$=2.656*10^{-25}\text{cm}^2$

$=0.2656\text{barn}$

To add the percentage error, main errors were happened from calculation of activity. When significant digits are used it also makes minor error. In average the percentage error in calculation of cross section is around 5.5% from activity measurement, around 3% from flux, random decay, efficiency calculation and other calculation, *total error* of 8.5% were seen. So the measured cross section will become;

$\sigma = 0.2656 \pm 8.5\% barn$

$\sigma = 0.2656 \pm 0.023 barn$

3.4. **Beta counting**

The values of capture cross section from the beta counts can also be found using the same equation Eq. [5]. The only change is since the beta counter does not differentiate the energy peaks it only gives the total counts of all the peaks. Hence no need of using the intensity of a particular energy of beta particle. Here, since the sample is the same, the number of atoms in each sample is the same with that of the first measurement. In this part of experiment the irradiation time was very short as compared to the first experiment (only less than $4h_r$). So beta energy of short half life will be expected which defines properties of Br-79.

3.4.1. *GM-Counter*

A Geiger counter (Geiger-Muller tube) is a device used for the detection and measurement of all types of radiation: alpha, beta and gamma radiation. Basically it consists of a pair of electrodes surrounded by a gas. The electrodes have a high voltage across them. The gas used is usually Helium or Argon. So beta counter is a GM-counter having small size, in order to prevent the back ground radiations that falls on its body. When radiation enters the tube it can ionize the gas. The ions (and electrons) are attracted to the electrodes and an electric current is produced. A scalar counts the current pulses, and one obtains a "count" whenever radiation ionizes the gas.

A typical beta counter consists of a tube having a thin mica end-window, a voltage supply for the tube, a scalar to record the number of particles detected by the tube, and a timer which will stop the action of the scalar at the end of a preset interval. This apparatus consists of two parts, the tube and the counter + power supply as seen in Fig. 9 [9].

3.4.2. *Materials used in beta counting*

- beta detector
- GM-counter
- sample holder
- connecting wires
- stop watch
- DC power supply
- blocks of detector covering leads

3.4.3. *Beta counter set up*

Fig. 9 Beta counter set up

3.4.4. *Beta counting procedure*

GM counter is connected to a power supply and beta detector is cascaded with it. Beta detector is placed in a blocks of lead to minimize the back ground radiation where sample placement is labeled under the detector. The samples are placed close to detector as much as possible to minimize beta absorption. After samples removed from radiation source by noting time, it brought to the detector as fast as possible to minimize the decay time and placed on the sample holder and putted close to window of detector. Then count will started by noting the time for the needed seconds which is pre sated (100sec), here data taking is manual not as gamma detector in which every things are recorded by computer. The operating voltage of GM-counter is also pre adjusted on 450kV and GM-counter works normally.

Readings are taken until reading with presence of sample is the same with back ground reading such that the decay of sample is seen clearly for each sample consecutively.

Activation of KI

Thermal neutron reaction with the KI target results in (n,γ) reaction with that of I-127 metallic element;

$$n+^{127}I \dashrightarrow [^{128}I]^{*} \dashrightarrow Xe+\beta^{-}+\upsilon+2119keV(93.1percent)$$

$$\dashrightarrow [^{128}I]^{*} \dashrightarrow Te+\bar{\upsilon}+1252keV(6.9percent)$$

The excited iodine [^{128}I] de-excited to the ground level of Xe atom by emitting five types of beta particles having the following end point energy and branching ratio [9].

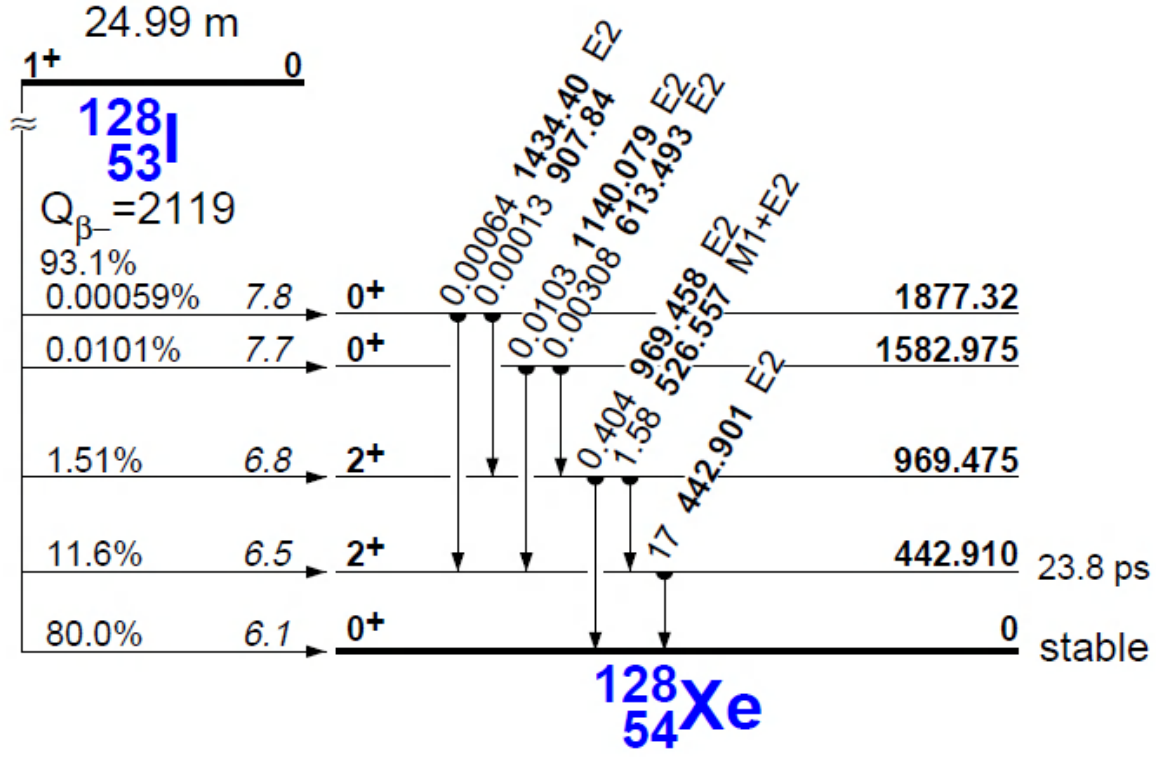

Fig.10 Decay scheme of I-128

$$\beta_1 \dashrightarrow 2119keV \dashrightarrow 80percent$$

$$\beta_2 \dashrightarrow 1676keV \dashrightarrow 11.6percent$$

$$\beta_3 \dashrightarrow 1149.5keV \dashrightarrow 1.51percent$$

$$\beta_4 \dashrightarrow 536keV \dashrightarrow 0.01percent$$

$$\beta_5 \dashrightarrow 241.68keV \dashrightarrow 0.00056percent$$

Activation of Br-79

When Br-79 bombarded by slow neutrons, it emits betas with a half life of 17.68 minutes, end point energy of 2.004Mev and gamma with very short life time. The thermal neutron capture cross- section is 8.6±0.4 barns as given in ref.[20].

Now we have suitable nuclide in Br-79, of neutron bombardment leads to short lived activities and the decay curve can be drawn when the count rate of a GM counter is plotted against decay time. The reaction produced by the neutron is:

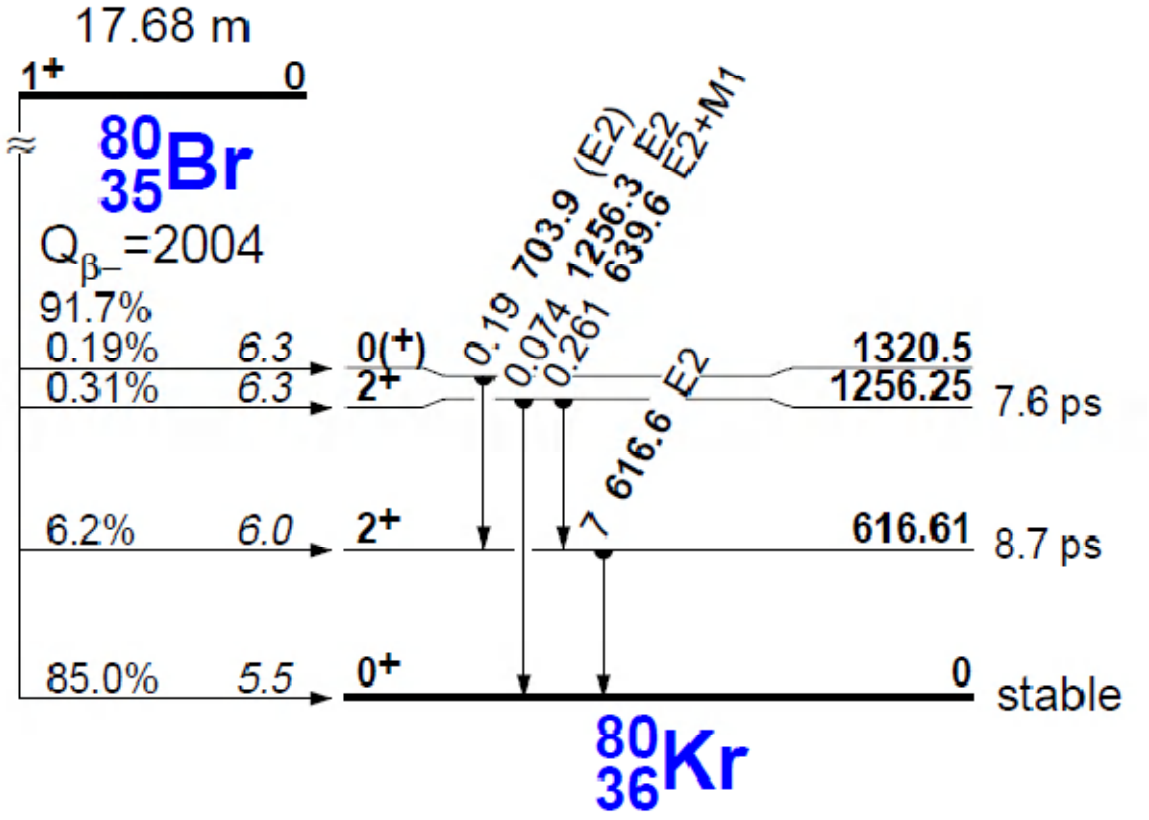

Fig.11 Decay scheme of Br-82

$$n+^{79}Br --> ^{80}Br + \gamma(prompt) --> ^{80}Br + \beta^{-} + \gamma(delayed)(E_{\max} = 2.004MeV, t_{1/2} = 17.68\,\min)$$

$$\beta_1 ---> 2004keV ---> 85\,percent$$

$$\beta_2 ---> 1.387keV ---> 6.2\,percent$$

$$\beta_3 ---> 0.7477keV ---> 0.31\,percent$$

$$\beta_4 ---> 0.6835keV ---> 0.19\,percent$$ [21]

3.4.5. ***Measurements of beta particles***

Back ground measurement

Since the environment is dynamic measurement of back ground is not the same. So several measurements were taken and the mean value of back ground was subtracted from the sample readings which is 22 counts/100sec.

Decay time(sec)	Activity(count/100sec)	±√(count/100sec)
300	125	11.18
760	116	10.77
1180	92	9.59
1590	47	6.85
2018	45	6.71
2465	35	5.92
2915	42	6.48
3397	25	5
3695	33	5.74
4205	32	5.66
4855	12	3.46
5415	7	2.65
6025	5	2.24
6540	8	2.83
7165	7	2.65
9580	3	1.73
11210	5	2.24
14530	4	2
16540	3	1.73

Table.8 Decay table of front KI target

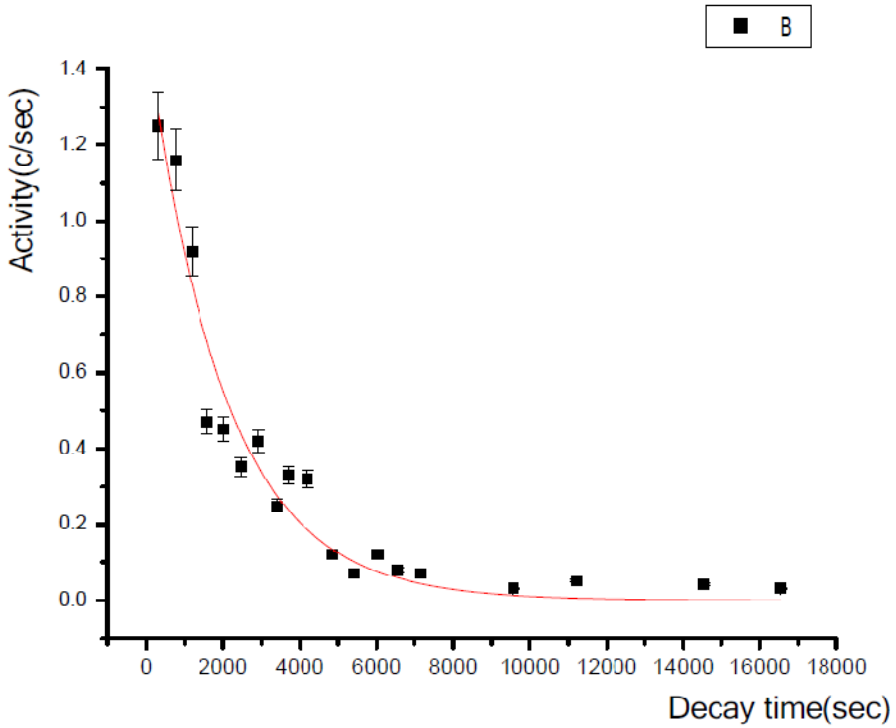

Graph.12 Exponential decay curve of front KI target

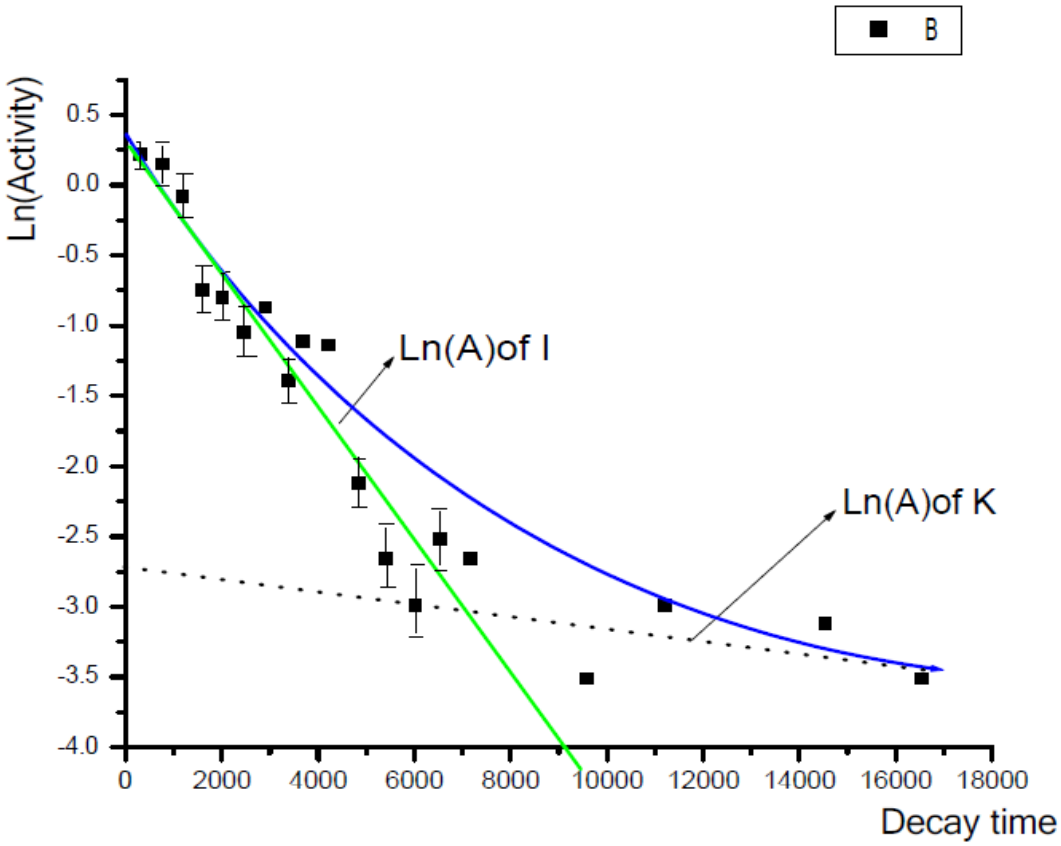

Graph.13 Logarithmic decay curve of front KI target

Decay time(sec)	Activity(count/100sec)	±√(count/100sec)
470	112	10.58
889	93	9.64
1312	66	8.12
1732	47	6.86
2170	45	6.71
2615	53	7.28
3076	47	6.86
3545	16	4
3870	24	4.9
4355	19	4.36
5028	13	3.6
5590	24	4.9
6195	4	2
6700	5	2.24
7320	12	3.46
8525	8	2.83
9720	3	1.73
11020	5	2.24
14100	4	2
16650	3	1.73

Table.9 Decay table of back KI target

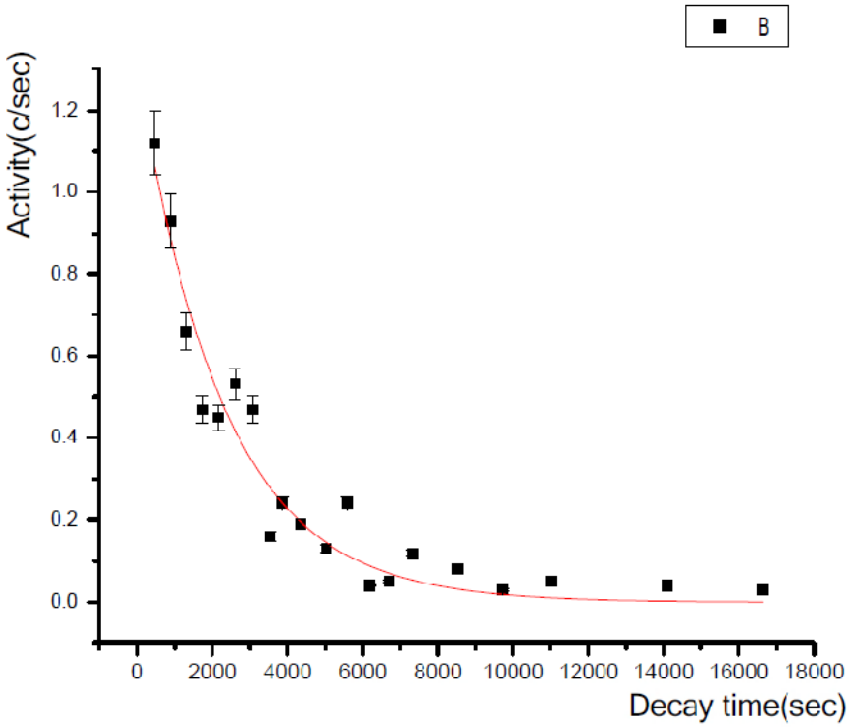

Graph.14 Exponential decay curve of back KI target

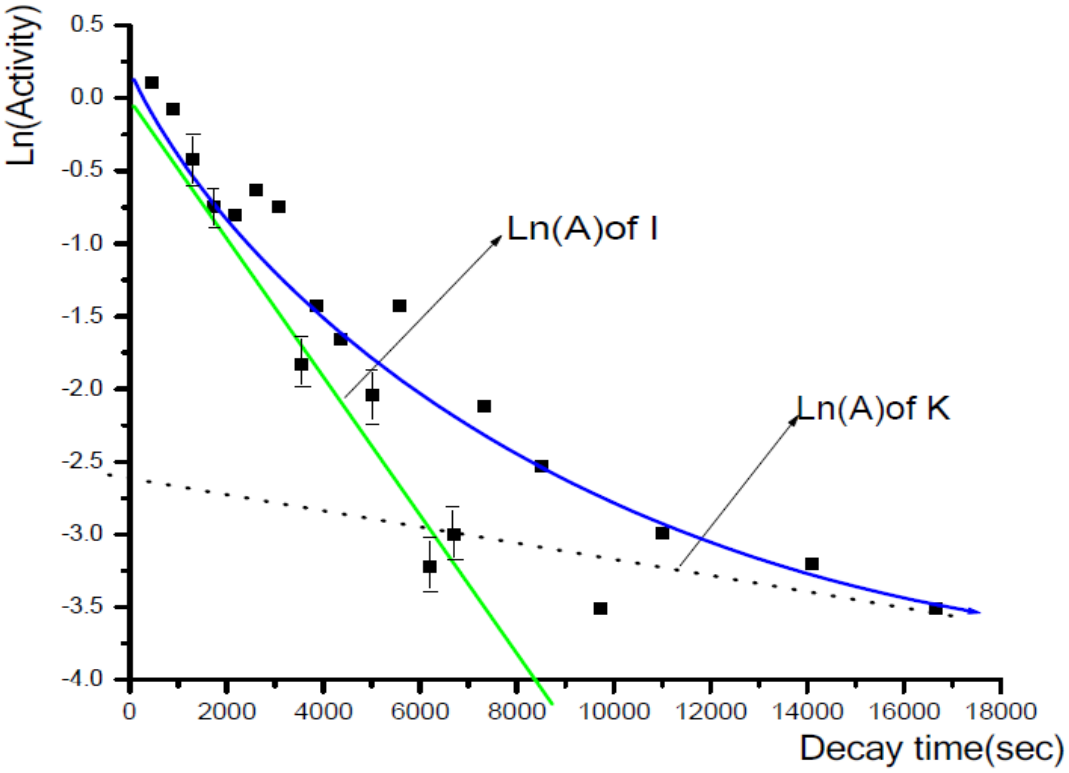

Graph.15 Logarithmic decay curve of back KI target

Decay time(sec)	Activity(count/100sec)	±√(count/100sec)
120	125	11.18
605	88	9.38
1032	65	8.06
1450	45	6.71
1877	60	7.75
2315	35	5.92
2762	50	7.07
3250	35	5.92
4055	18	4.24
4372	16	4
4700	17	4.12
5236	22	4.69
5860	8	2.83
6380	9	3
6855	12	3.46
7855	6	2.45
8805	8	2.83
8950	5	2.24
9275	3	1.73

Table.10 Decay table of Br-80

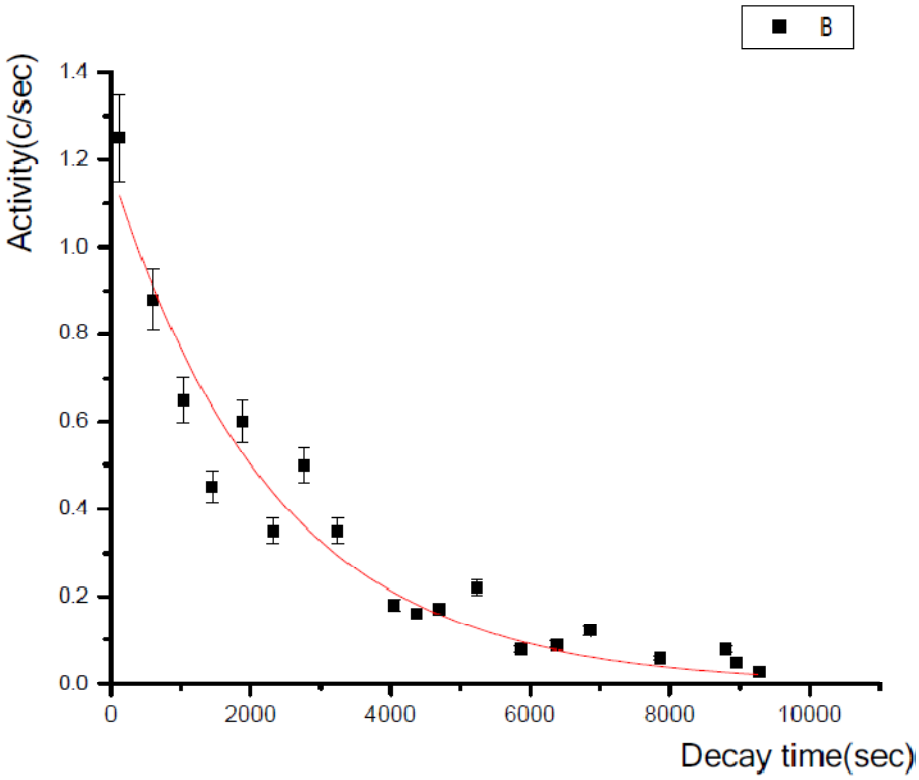

Graph.16 Exponential decay curve of Br-80

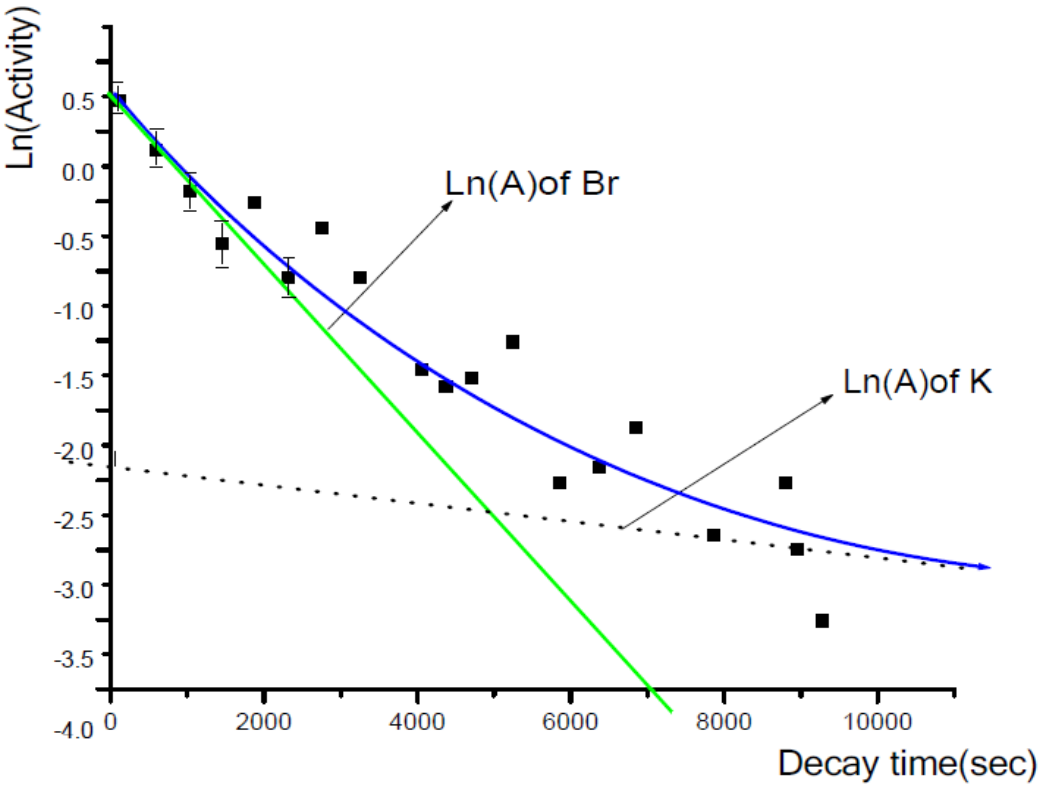

Graph.17 Logarithmic decay curve of Br-80

3.4.6. ***Result and discussion***

Activities are now easy to calculate from the above graphs. The flux of thermal neutron is also calculated from the activity obtained by using the above equation and decay constants are used from reference as in first calculation.

$$\phi = \frac{(dn/dt)}{N_0 \sigma \varepsilon (1-\exp(-\lambda t_1))(1-\exp(-\lambda t_3))}$$

Here t_2 is not included in the calculation because activities are determined at t_2=0 and only t_1 and t_3 survive. i.e $(1-e^{-(4.63*10\text{^-}4*13020)})$=0.9976≈1 for t_1 and$(1-e^{-(4.63*10\text{^-}4*100)})$=0.045 for t_3.

dn/dt=1.28dps at t_d=0, from graph [13]

Efficiency is calculated by using;

$$\varepsilon = [ae^{-\mu_1 d} + be^{-\mu_2 d} + ce^{-\mu_3 d} + fe^{-\mu_4 d} + ge^{-\mu_5 d}] \quad 59$$

Where a,b,c,f and g are beta branching ratio of iodine (80,11.6,1.5,0.01,0.00056 percent respectively) from fig. [10];

$$d = d_1 + d_2 + d_3 \quad 60$$

d_1 is thickness of the tape (0.0025g/cm^2)

d_2 is thickness of beta counter window (0.002g/cm^2)

d_3 is half thickness of sample;

$$d_3 = \frac{1}{2}\frac{measuredmass}{areaofsampleholder} \quad 61$$

d_3 = 0.5*0.1985g/0.95cm^2=0.104g/cm^2 for front iodine,

d=0.11g/cm^2

μ_m (mass absorption coefficient) is calculated by using the empirical relation

$$\mu_m = 17[E]^{-1.14} \quad 62$$

[9]

E is the end point energy of beta.[fig.11]

μ_{m1}=17[2.119]$^{-1.14}$=7.22cm^2/g

μ_{m2}=17[1.676]$^{-1.14}$=9.4cm^2/g

μ_{m3}=17[1.149]$^{-1.14}$=14.5cm^2/g

μ_{m4}=17[0.536]$^{-1.14}$=34.6cm^2/g

μ_{m5}=17[0.241]$^{-1.14}$=86cm^2/g

by putting all these quantities in eq. [58]

$$\varepsilon = [0.8e^{-0.79} + 0.116e^{-1.03} + 0.015e^{-1.6} + 0.0001e^{-3.8} + 0.0000056e^{-9.46}] = 0.39$$

So using all this information when we calculate thermal neutron flux for the front iodine;

$$\phi_1 = \frac{1.28dps}{7.12*10^{20}atoms*6.2*10^{-24}cm^2*0.39*0.045} = 1.65*10^4 n/cm^2 \sec$$

For back thermal neutron flux the changed parameters are half thickness of sample, activity and number of atoms only. So d_3 becomes now;

d_3=0.5*0.6192g/0.95cm^2=0.326g/cm^2

d=d_1+d_2+d_3=0.33g/cm^2, where d_1 and d_2 are as given in flux one calculation.

$$\varepsilon = [0.8e^{-2.3} + 0.116e^{-3.1} + 0.015e^{-4.9} + 0.0001e^{-11.4} + 0.0000056e^{-28.86}] = 0.088$$

dn/dt=0.86dps, from graph[15]

$$\phi_2 = \frac{0.86dps}{2.22*10^{21}atoms*6.2*10^{-24}cm^2*0.088*0.045} = 1.57*10^4 n/cm^2 \sec$$

The average neutron flux captured by the two iodine samples calculated as;

$$\Phi = \frac{\phi_1 + \phi_2}{2} = 1.61*10^4 \text{n/cm}^2\text{sec}$$

3.4.7. *Neutron Capture Cross-Section in Br-79*

To evaluate neutron capture cross section by beta counter, simply by rearranging the flux equation, where (1-e$^{-(6.4*10\text{^-}4*13020)}$)=0.99976≈1for t_1 and (1-e$^{-(6.4*10\text{^-}4*100)}$)=0.06 for t_3.

$$\sigma = \frac{(dn/dt)}{N_0\phi\varepsilon(1-\exp(-\lambda t_1))(1-\exp(-\lambda t_3))}$$

When Br-80 decays to Kr-80 it emits 4 types of beta particles with different branching ratio. So to calculate efficiency by using fig [11];

$$\varepsilon = [ae^{-\mu_1 d} + be^{-\mu_2 d} + ce^{-\mu_3 d} + fe^{-\mu_4 d}]$$

Where a,b,c,f are beta branching ratio of Br-80 with 0.85,0.062,0.0031 and 0.0019 percent value respectively.

d is calculated in same as in eq. [60], where d_3 is also calculated in same way.

D_3=0.5*0.1739g/0.95cm^2=0.09g/cm^2

D=d_1+d_2+d_3=0.0945g/cm^2

$\mu_{m1}=17[2.004]^{-1.14}=7.1cm^2/g$

$\mu_{m2}=17[1.3874]^{-1.14}=11.7cm^2/g$

$\mu_{m3}=17[0.747]^{-1.14}=23.7cm^2/g$

$\mu_{m4}=17[0.6835]^{-1.14}=26.236cm^2/g$

$$\varepsilon=[0.85e^{-67}+0.062e^{-1.1}+0.0031e^{-2.24}+0.0019e^{-2.48}]=0.44$$

dn/dt=1.6dps, from graph[14]

$$N_3=\frac{79g/mole*0.1739g}{122g/mole}*0.5069\frac{6.023*10^{23}atoms/mole}{79g/mole}=4.35*10^{20}atoms$$

$$\sigma=\frac{1.6dps}{4.35*10^{20}atoms*1.61*10^{4}n/cm^2\sec 0.44*0.06}$$

$=8.653*10^{-24}cm^2$

$=8.653barn$

In this calculation there are so many sources of errors and percentage of error is added as in the previous calculation. From all calculations *total percentage error* of 9% was appeared. So the measured thermal neutron capture cross section by beta counter becomes;

$\sigma=8.653\pm 9\%\ barn$

$\sigma=8.653\pm 0.78\ barn$

3.4.8. *Comparison of experimental result with Theoretical valeus*

Having the above two measurements, that is for the ground state thermal neutron cross section of Br-79 and Br-81 and with the meta stable state cross section in ref [20]; when we calculate the theoretical resonance thermal neutron cross section of s-wave;

For Br-79 the total measured thermal neutron cross section is [meta stable state (2.4b) and ground state ($8.653b^*$)], 11.0±0.7 barn.[20]

When we calculate theoretically based on the idea in section 2.7.4., in above;

I=3/2., by using equation [48], g=0.625/0.375

Having this and eq. [50] S_0 becomes;

$S_0=0.625*10^{-4}/0.375*10^{-4}$ or av. $S_0=0.5*10^{-4}$.

using eq.[54] where Γ_γ =0.313±5eV, D_0=53.8±2.8eV [17];

$$S_{0\gamma}=\frac{0.313}{53.8}=5.8*10^{-3}$$

$$\sigma_\gamma^*=0.404*10^8(\frac{79+1}{79})^2*(0.5*10^{-4})*5.8*10^{-3}=11\pm 2.96 barn$$

In the same way, for Br-81 the total measured values [meta stable state (2.43b) and ground state (0.26)] of thermal neutron cross section is 2.7±0.2barn. [20]

Here, values of S_0 is the same, and when we calculate for $s_{\gamma 0}$, where Γ_γ=0.243±5eV, D_0=145±8eV [17];

$$S_{0\gamma}=\frac{0.243}{145}=1.68*10^{-3}$$

$$\sigma_\gamma^*=0.404*10^8(\frac{80+1}{80})^2*(0.5*10^{-4})*1.68*10^{-3}=3.39\pm 0.85 barn$$

In my calculation, the calculated resonance thermal neutron cross section coincides with the measured values in ref. [20], so statistical estimates of thermal neutron cross section is applicable in determining thermal neutron cross sections of elements.

Chapter Four

Sources of Errors and Conclusion

4.1) **Sources of Errors**

In this experiment the measurement consists of measuring the photo peak area of gamma ray emitted from induced radioactive element and counting the number of emitted ß$^-$ during a definite time interval (t_3).There are two types of source of errors expected in the experiment. These are;

a) Errors in the Measurement

The possible source of systematic and random source of errors in the measurement process contains; personal errors in using significant digits, photo peak area measurement in gamma counting, in measuring time interval, placement of samples at the center of detectors, and back ground measurements especially in beta counting takes major sources of errors in the above measurements. Error in the measurement takes more than half of the total error in the obtained results.

b) Errors due to Random Nature of Decay Process

This is the randomness of the decay process or in the decay data distribution that has nothing to do with the measurement process. There exist for any radioactive substance a certain probability that any particular nucleus will emit radiation within a given time interval. This is the same for all nuclei of the same type. Here, we cannot predict the time at which an individual nucleus will decay. However, when there is a large number of disintegration takes place, there is a definite average decay rate which is the characteristic for a particular nuclei type, but the actual number of decaying in any specific interval may vary significantly from the average value. Thus, there may not be correct answer to which we can compare our experimental findings. We can emphasis that these errors cannot be removed by improving the precession of the experiment but it can be improved only at the expense of significantly increasing the time duration of the counting.

By considering all these sources of errors the error in this measurement by comparing with that of listed in literature is the previously determined capture cross section of Br-82, in literature [20] is 0.26 barns. The value of capture cross section in this experiment is 0.2656 barns.

The error in this case from the value in literature is;

Error(%)=|(previous value-measured value)/ previous value | *100 63

Error(%)=|(0.26-0.2656)/0.26|*100

=2.15%

In the same way the previous determined capture cross section of Br-80 in literature is 8.6 barns, where as in measurement it was 8.653 barns.

Error (%)=|(8.6-8.653)/8.6|*100

=0.62%

The result of this work suggests that, using Instrumental Neutron Activation Analysis technique it is possible to perform environmental radio-analysis with an improved counter shielding and good precision of measurement. This may very important to elemental analysis of a given sample of interest in the fields of like, medicine, forensic, mining, industry and any other applications.

4.2. Conclusion

Instrumental Neutron activation Analysis using Am-Be neutron source has profound effect in identifying the type of given element of sample. Here in this work, neutron capture cross section was measured and was compared with already known value. Also theoretical value was calculated using statistical formula. All these values were very close, within experimental error.

References

1) Robert Celotta and Judah Levine, Editors, Methods of experimental physics volume 23,_ Neutron scattering, Harcourt Brace Jovanovich, (AP_1986-1987)

2) Rauss_P,- Neutron physics, Institution of science EDP (2008)

3) Claude_Leray,_Pier_Giorgio_Rancoita_Principles_Of_Radiation_Interaction_In matter_ And_ Detection-World_Scientific_publishing_campany (2004)

4) **Benchtop Powder XRD** - Low-cost X-ray Diffraction system quantitative phase & crystallinity - www.rigaku.com

5) Pollard, A. M., Heron, C., *Archaeological Chemistry*. Cambridge, Royal Society of Chemistry (1996).

6) neutron-activation-analysis-naa- Ultra-Trace Bulk Analysis of Polysilicon by Instrumental Neutron Activation Analysis – http://www.google.htm

7) Michael D. Glascock, Neutron Activation Analysis, Elemental Analysis, Inc (2001)

8) Nelson Eby, Instrumental Neutron Activation Analysis (INAA) Geochemical Instrumentation and Analysis society (2011)

9) Tamene Hailu Melkegna Thermal Neutron Induced Reaction In As-75, AAU, Un published (2009)

10) Dr. Tarek Nagla-nuclear_engineering Library of Congress (2010)

11) J.B. Marion And J.L Fowler_Fast Neutron Physics Part I, Inter Science Publishers, London (1960)

12**)** Jeffrey S. Nico And W. Michael Snow_Experiments in Fundamental Neutron Physics, OHIO University Libraries (2006)

13) Elmer E. Lewis_Fundamentals of Nuclear Reactor Physics (2008)

14) U.S. Department Of Energy Washington, D.C. 20585_ Doe Fundamentals handbook_Nuclear Physics And Reactor Theory Volume 1 Of 2, (2010)

15) Yu. V. Petrov and A. I. Shlyakhter_ The Distribution of Thermal Neutron Cross Sections, Nuclear Physics Institute (1980)

16) Yu. V. Petrov and A. I. Shlyakhter_ Statistical Estimates of Thermal Neutron Capture Cross Sections, Nuclear Physics Institute (1984)

17) S.F. Mughabghab,

Atlas_of_Neutron_Resonances_Fifth_Edition_Resonance_parameters_and_Thermal_cross section Z_1-100 (2006)

18) Zeef_Alfassi,_Chien_Chung_Prompt_Gamma_Activation_Analysis, John Wiley and Sons, Inc. (1995)

19) Radiation Detector- http://www.ortec-online.com/papers/la_ur_03_4020.pdf

20) Handbook on Nuclear Activation Data, International Atomic Energy Agency (1987)

21) Richard B. Firestone_Tables_Of_Isotopes _Eighth_Edition (1999)

Declaration

This thesis is my original work, has not been presented for a degree in any other University and that all the sources of material used for the thesis have been brightly acknowledged.

Name: Hailu Geremew

Signature: ----------

Place and time of submission: Addis Ababa University, March 2012

.....

This thesis has been submitted for examination with my approval as University advisor.

Name: Prof. A.K. CHAUBEY

Signature: ----------